NASA TECHNICAL NOTE

NASA TN D-5621

$\mathcal{c}.\,/$

NASA TN D-5621

GASEOUS-HELIUM REQUIREMENTS FOR
THE DISCHARGE OF LIQUID HYDROGEN
FROM A 1.52-METER- (5-FT-)
DIAMETER SPHERICAL TANK

by Robert J. Stochl, Joseph E. Maloy, Phillip A. Masters,
and Richard L. DeWitt

Lewis Research Center
Cleveland, Ohio

NATIONAL AERONAUTICS AND SPACE ADMINISTRATION • WASHINGTON, D. C. • JANUARY 1970

1. Report No. NASA TN D-5621	2. Government Accession No.	3. Recipient's Catalog No.
4. Title and Subtitle GASEOUS-HELIUM REQUIREMENTS FOR THE DISCHARGE OF LIQUID HYDROGEN FROM A 1.52-METER- (5 FT-) DIAMETER SPHERICAL TANK		5. Report Date January 1970
		6. Performing Organization Code
7. Author(s) Robert J. Stochl, Joseph E. Maloy, Phillip A. Masters, and Richard L. DeWitt		8. Performing Organization Report No. E-4965
9. Performing Organization Name and Address Lewis Research Center National Aeronautics and Space Administration Cleveland, Ohio 44135		10. Work Unit No. 180-31
		11. Contract or Grant No.
		13. Type of Report and Period Covered
12. Sponsoring Agency Name and Address National Aeronautics and Space Administration Washington, D.C. 20546		Technical Note
		14. Sponsoring Agency Code

15. Supplementary Notes

16. Abstract

An experimental investigation was conducted to determine the effects of various physical parameters on the pressurant gas (helium) requirements during the pressurization and expulsion of liquid hydrogen from a 1.52-meter- (5-ft) diameter spherical tank. The experimental results show an average decrease in helium pressurant gas requirements of 1.3 percent for a 10 K (18° R) increase in inlet gas temperature. The analytical program was able to predict the actual pressurant requirements to within a maximum of 11.5 percent for all cases.

17. Key Words (Suggested by Author(s)) Pressurization Pressurized expulsion Gaseous helium pressurant Cryogenic propellant tanks	18. Distribution Statement Unclassified – unlimited		
19. Security Classif. (of this report) Unclassified	20. Security Classif. (of this page) Unclassified	21. No. of Pages 64	22. Price* $3.00

*For sale by the Clearinghouse for Federal Scientific and Technical Information
Springfield, Virginia 22151

CONTENTS

GASEOUS-HELIUM REQUIREMENTS FOR THE DISCHARGE OF LIQUID HYDROGEN

FROM A 1.52-METER- (5-FT-) DIAMETER SPHERICAL TANK

by Robert J. Stochl, Joseph E. Maloy, Phillip A. Masters, and Richard L. DeWitt

Lewis Research Center

SUMMARY

An experimental investigation was conducted to determine the effects of various physical parameters on the pressurant gas (gaseous helium) requirements during the pressurization and expulsion of liquid hydrogen from a 1.52-meter- (5-ft-) diameter spherical tank. The experimental results were compared with results predicted by a previously developed analytical program which was revised and extended for this investigation. Tests were conducted for a range of liquid outflow rates, pressurizing rates, and initial ullage volumes at a nominal operating pressure of 34.47×10^4 newtons per square meter (50 psia) using nominal inlet gas temperatures of 183, 267, and 322 K (329°, 480.6°, and 580° R). Data were obtained using a hemisphere injector.

The experimental results show that the inlet gas temperature has a strong influence on the actual pressurant gas requirements. There is an average decrease in pressurant gas requirements of 1.3 percent for a 10 K (18° R) increase in inlet gas temperature. The analytical program was able to predict the actual pressurant requirements to within a maximum error of 11.5 percent for all cases.

INTRODUCTION

During the past several years, a great deal of effort has been devoted to the problems associated with the pressurized discharge of a cryogenic liquid from a tank. The main objectives of these efforts have been toward the optimization of a propellant tank pressurization system. One phase of this optimization is a precise determination of pressurant requirements for any given set of operating parameters (i.e., tank pressure, inlet gas temperature, liquid outflow rate, tank size, etc.). This knowledge would allow the design of a system based on only the weight of gas necessary to accomplish the mission.

Several investigators have developed analyses (e.g., refs. 1 and 2) which attempt to predict, according to a selected set of simplifying assumptions, the quantity of pressurant gas required during the pressurized discharge of liquid hydrogen (LH_2). Some of these simplifying assumptions may, for certain conditions (i.e., for various injector geometries, tank shapes, and tank sizes), limit the capability of the analysis to predict pressurant requirements accurately. Because of these limitations, the validity of the analytical results have to be largely based on correlations with experimental results.

An experimental investigation was started at Lewis Research Center to determine the effects of various physical parameters on the pressurant gas requirements during the pressurization and expulsion of liquid hydrogen from propellant tanks. The experimental results were also used to extend the capability of the analysis of reference 1 to predict the pressurant requirements for tanks of general size and geometry under various operating conditions. Some results of this program, which used hydrogen gas as the pressurant, are reported in references 3 to 5. In general, the experimental results reported in references 3 to 5 indicate that the temperature of the inlet gas, the injector geometry, and the tank pressure have a strong influence on the pressurant gas requirements. There was between a 1.2 and 1.4 percent decrease in pressurant requirement for a 10 K (18° R) increase in the temperature of the inlet gas depending on liquid outflow rate and tank size. These data also indicate that the use of a straight pipe injector could reduce the pressurant requirement by 9 to 35 percent, depending on liquid outflow rate and tank size, compared with that obtained using diffuser-type injectors. It was also shown that pressurant requirements increased in proportion to increased tank pressure level.

The analysis of reference 1 was used to predict the pressurant requirements in references 3 to 5. It was modified in references 4 and 5 to accommodate a spherical tank geometry and also to include the heat transfer from the gas to the liquid surface (which was neglected in the original analysis). The analysis predicted the actual pressurant re-quirements for the various operating parameters within 12.4 percent with the exception of the tests performed with the straight pipe injector. The analysis overpredicted the pressurant requirements for the straight pipe injector by as much as 45 percent.

If only pressurant gas weight is considered, it appears advantageous to use hydrogen (because of its low molecular weight) as the pressurant for the expulsion of liquid hydrogen. Since gaseous hydrogen cannot be used as the pressurant for most oxidizers and a dual pressurization system would probably result in an additional payload penalty, it would appear desirable to use a single pressurant gas which is compatible with liquid hydrogen and any oxidizer. To meet this requirement, helium is the only logical choice because it has a low molecular weight and, since it is an inert gas, it is compatible with any fuel-oxidizer combination.

This report presents the results obtained using gaseous helium as the pressurant for the expulsion of liquid hydrogen. The use of helium as a pressurant in the expulsion of

liquid hydrogen adds further complication to both the analytical and experimental programs. The ullage volume for this system contains a binary gas, part of which is condensable and part is not. The analytical model must either (1) account for the possibility of a binary gas in the ullage volume by diffusion and/or evaporation or (2) assume the contribution of hydrogen to the ullage volume to be small enough that the ullage can be considered at 100 percent helium at all times, except at the interface where it is considered to be 100 percent hydrogen. The analysis used in this report is identical to that used in reference 4 with the exception that this analysis treats the ullage volume as if it contained pure helium. (For convenience, the modifications to the analysis of ref. 1 that were used in ref. 4 are presented in appendixes A, B, and C.) Experimentally measured gas concentration gradients in the ullage volume were used to obtain mass and energy balances and to verify the 100 percent helium model used in the analysis.

The primary objective of the test work described herein was to obtain experimental values on the helium pressurant gas requirements during the initial pressurization and expulsion periods for the various operating parameters and to compare these values with predicted ones. A secondary objective was to obtain experimental information on tank wall heating, liquid heating, residual ullage energy, and mass transfer in order to gain an insight into the reasons for any variations in pressurant gas requirements.

The tests were conducted using the same two 1.52-meter- (5-ft-) diameter spherical aluminum tanks that were used in reference 4. The pressurant used for this series of tests was gaseous helium. The main test variables were (1) tank wall thickness (0.762 and 0.409 cm; 0.30 and 0.161 in.), (2) nominal inlet gas temperatures of 183, 267, and 322 K (329°, 480.6°, and 580° R), (3) liquid outflow rates between 0.282 and 0.824 kilogram per second (0.623 and 1.817 lb/sec), and (4) initial tank ullages of 4, 28, 55, and 75 percent. Data were also obtained for pressurization of the tank at various rates $(3.24 \times 10^3$ to 11.37×10^3 $(\text{N/m}^2)/\text{sec}$; 0.47 to 1.65 psi/sec) from 1 atmosphere to the desired operating level. All tests were performed at a nominal operating tank pressure of 34.47×10^4 newtons per square meter (50 psia).

SYMBOLS

A   area, m^2 (ft^2)

b $1 - \dfrac{z_1}{z} - 2\dfrac{\Delta r}{r_i}$

C   orifice coefficient

C_H effective perimeter of interior hardware, m (ft)

C_p specific heat at constant pressure, J/(kg)(K)   (Btu/(lb)(°R))

C_v specific heat at constant volume, J/(kg)(K)   (Btu/(lb)(^{O}R))

C_w specific heat of tank wall, J/(kg)(K)   (Btu/(lb)(^{O}R))

c $\alpha - \alpha\omega - T_w - \dfrac{1}{l_w \rho_w} \Delta t \dfrac{\dot{q}}{C_w}$

D   orifice diameter, m (ft)

d $\dfrac{Z_2}{Z} \dfrac{\Delta X}{\Delta t} \dfrac{P' - P}{P'} - \dfrac{Z_1}{Z} \dfrac{\Delta X}{\Delta t}$

Gr   Grashof number, $\dfrac{L^3 \rho^2 g \beta \Delta T}{\mu^2}$

g   gravity acceleration, m/sec^2 (ft/sec^2)

H   enthalpy, J (Btu)

h   specific enthalpy, J/kg (Btu/lb)

h_c convective heat-transfer coefficient, J/(m^2)(K)(sec)   (Btu/(ft^2)(^{O}R)(sec))

k   thermal conductivity, J/(m)(K)(sec)   (Btu/(ft)(^{O}R)(sec))

L   flow length, m (ft)

l thickness, m (ft)

M   mass, kg (lb)

ΔM differential mass, kg (lb)

$\dot{M}$ mass flow rate, kg/sec (lb/sec)

$\overline{M}$ molecular weight, kg/(kg-mole)   (lb/(lb-mole))

M_I ideal pressurant requirement, kg (lb)

N   number of volume segments

$\overline{N}$ number of data points used in defining average deviation

$N_1 - N_z$ particular volume segments

Nu   Nusselt number, $h_c L/k$

n or i   summing index

P   pressure, N/m^2 (lb/in.^{2})

ΔP differential pressure, N/m^2 (lb/in.^{2})

ΔP^* orifice ΔP

Pr   Prandtl number, $\mu C_p/k$

4

Q	heat transfer, J (Btu)
$\dot{Q}$	heat-transfer rate, J/sec (Btu/sec)
$\dot{Q}'$	specific heat-transfer rate, J/(kg)(sec) (Btu/(lb)(sec))
$\dot{q}$	heat-transfer rate per unit area, J/(m^2)(sec) (Btu/(ft^2)(sec))
R	gas constant, J/(K)(kg-mole) (Btu/(^{O}R)(lb-mole))
r	radius, m (ft)
Δr	increment of radius, m (ft)
Re	Reynolds number, $L\bar{V}\rho/\mu$
ΔS	increment of arc length, m (ft)
T	temperature, K (^{O}R)
ΔT	differential temperature, K (^{O}R)
T_δ	temperature at the edge of thermal boundary layer, K (^{O}R)
t	time, sec
Δt	time increment, sec
U	internal energy, J (Btu)
ΔU	differential energy, J (Btu)
u	specific internal energy, J/kg (Btu/lb)
V	volume, m^3 (ft^3)
ΔV	volume increment, m^3 (ft^3)
$\bar{V}$	velocity, m/sec (ft/sec)
v	specific volume, m^3/kg (ft^3/lb)
W	work, J (Btu)
X	percent of gas by volume
X_n	number of net points in the ullage
x	coordinate in direction of tank axis, m (ft)
Δx	space increment, m (ft)
Y	expansion factor
y	thickness within the boundary layer, m (ft)
Z	compressibility factor
z	elevation or vertical distance along tank wall, m (ft)

$$\alpha \qquad \dfrac{1 + \dfrac{h_c\,\Delta t}{\rho_w \ell_w C_w}}{\left(\dfrac{2h_c RZ\,\Delta t}{r\overline{M}PC_p}\right)\left[1 + \left(\dfrac{\Delta r}{\Delta x}\right)^2\right]^{1/2}}$$

β coefficient of thermal expansion, $1/K$ $(1/^{O}R)$

γ specific heat ratio

δ finite increment, or total boundary layer thickness, m (ft)

λ latent heat of vaporization, J/kg (Btu/lb)

μ viscosity, kg/(m)(hr)   (lb/(ft)(hr))

ρ density, kg/m^3 (lb/ft^3)

ω $\left(\dfrac{R}{\overline{M}}\, Z_1\, \dfrac{\Delta P}{\Delta t} + \dfrac{RZC_H}{\overline{M}\pi r^2}\,\dot{q}_H\right)\dfrac{\Delta t}{C_p P}$

Subscripts:

A   analytical results

ad   adiabatic

E   experimental results

f   final state or condition

G   gas added to tank

H   internal hardware

He   helium

H_2 hydrogen

i   initial state or condition

i → f   from initial to final state or condition

L   liquid

n   summing index

o   condition prior to ramp

S   liquid surface

sat   saturation

T   total quantity

6

t   transferred

t_1, t_2 times 1 and 2

U   ullage

w   wall

Superscripts:

'   time index

*   evaluation may be performed at beginning or end of time interval

Constants for Beattie-Bridgeman equation:

A $(N)(m^4)/kg^2$ (ft^4/lb)

a m^3/kg (ft^3/lb)

B m^3/kg (ft^3/lb)

b m^3/kg (ft^3/lb)

C $(m^3)(K^3)/kg$ $((ft^3)(^{\circ}R^3)/lb)$

$\overline{M}'$ $X_{H_2}\overline{M}_{H_2} + X_{He}\overline{M}_{He}$

ϵ $\dfrac{X_{H_2}C_{H_2} + X_{He}C_{He}}{vT^3}$

APPARATUS AND INSTRUMENTATION

Facility

All tests were conducted under vacuum inside a 7.61-meter- (25-ft-) diameter spherical vacuum chamber (fig. 1) to reduce the external heat leak into the propellant tank to a low value. The vacuum capability of this chamber was approximately 8×10^{-7} mm Hg. A general schematic of the test tank and associated equipment is shown in figure 2. A heat exchanger and blend valve subsystem capable of delivering gaseous helium at any desired temperature between 167 and 405 K (301° and 729° R) at a maximum flow rate of 9.98×10^{-2} kilogram per second (0.22 lb/sec) was used to control pressurant gas inlet temperature. A ramp generator and control valve were used for controlling the initial rate of pressurization of the propellant tank. A closed-loop pressure control circuit was
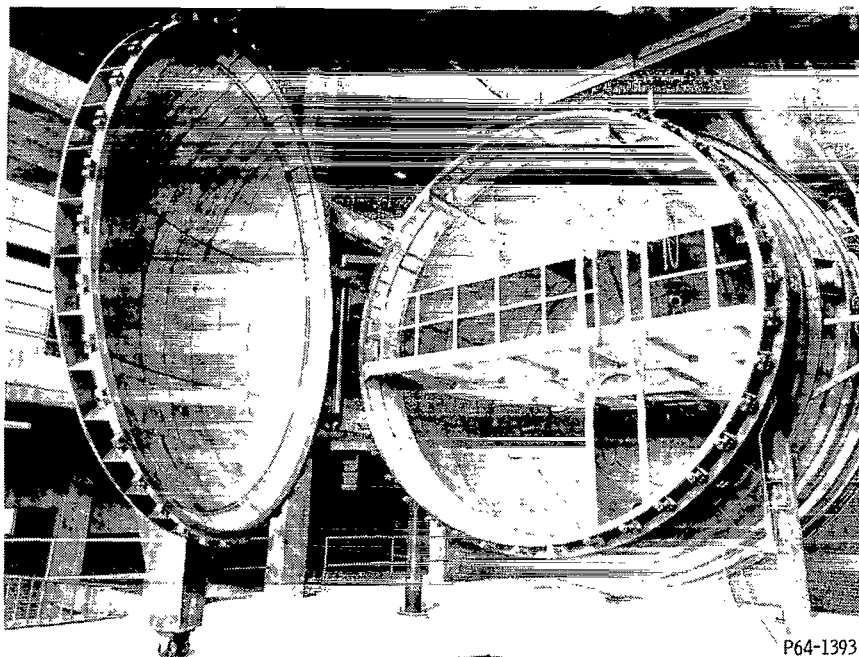
Figure 1. - 7.61-Meter- (25-ft-) diameter vacuum chamber.

used to maintain constant tank pressure during the expulsion period. The liquid outflow rate was controlled by remotely operated variable flow valves. The liquid hydrogen outflow from the tank was returned to the storage Dewar.

Liquid outflow rates were measured using a turbine-type flowmeter located in the transfer line. The flowmeter was calibrated (within an estimated uncertainty of $\pm 1/2$ percent) with liquid hydrogen over the expected range of flow rates. The calibration was performed at Lewis. Pressurant gas inlet flow rates were determined by the use of an orifice located in the pressurant supply line. Tank, line, and differential pressures were measured with bonded strain-gage-type transducers (estimated uncertainty, $\pm 1/4$ percent).

Test Tanks

The experimental work was conducted in 1.52-meter- (5-ft-) diameter bare wall spherical aluminum tanks. One tank (fig. 3) had an average wall thickness of 0.762 centimeter (0.30 in.). The other tank was identical except the wall was chem-milled down to an average thickness of 0.409 centimeter (0.161 in.). One stainless steel lid served both tanks. The lid housed the inlet and vent pipes and the electrical connections for all internal tank instrumentation. The lid was 0.457 meter (18 in.) in diameter, 3.18 centi-

8
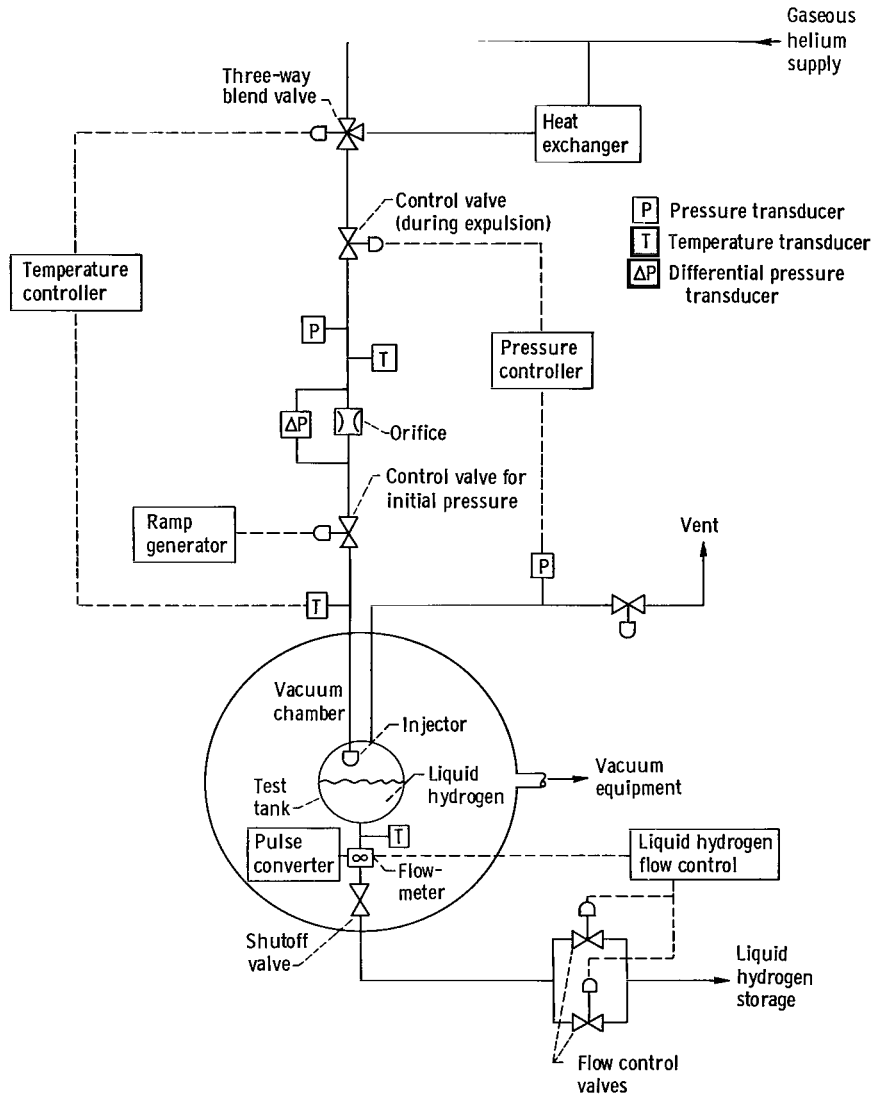
Figure 2. - General schematic of facility.
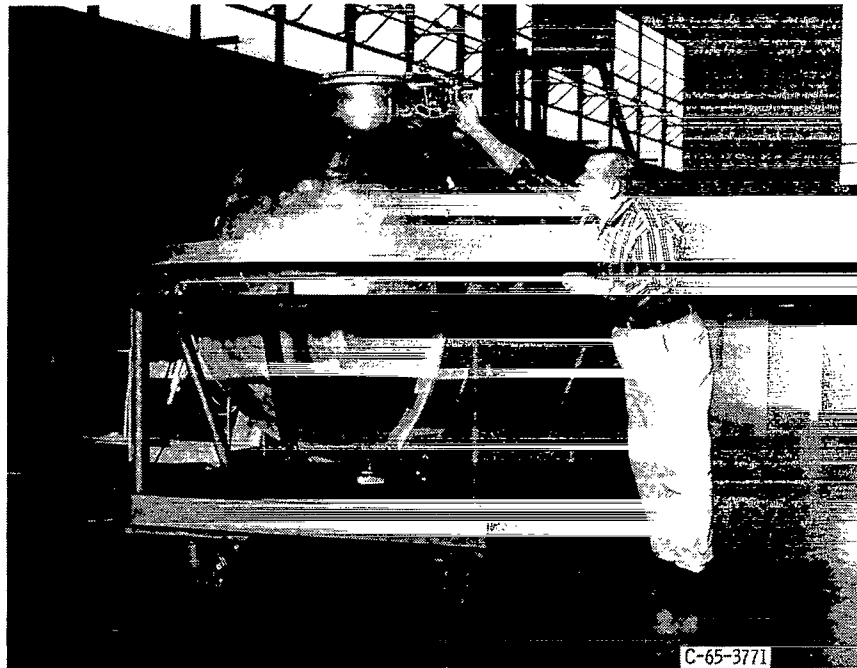
Figure 3. - 1.52-Meter- (5-ft-) diameter spherical test tank. Tank wall thickness, 0.762 centimeter (0.30 in.).

meters (1.25 in.) thick, and weighed 67.50 kilograms (149 lb). The inner surface of the lid conformed to the contour of the tank wall.

A viewport and television camera were installed on the 0.762-centimeter- (0.30-in.-) wall test tank (fig. 4) for the purpose of visually locating the initial liquid level in the tank prior to expulsion, and to enable observation of any physical processes occurring in the tank. Lighting of the tank interior was accomplished by bulbs mounted on the inner surface of the tank wall.

Pressurant Gas Injector Geometry

A hemisphere injector (fig. 5) was used for all tests reported herein. The hemisphere injector was selected because it injects the pressurant uniformly in all directions into the ullage volume (minimizes ullage gas mixing). The uniform diffusion of pressurant is a basic assumption of the analysis used in this report. The open exit area for the injector was 176.8 square centimeters (27.4 in.^{2}).

10
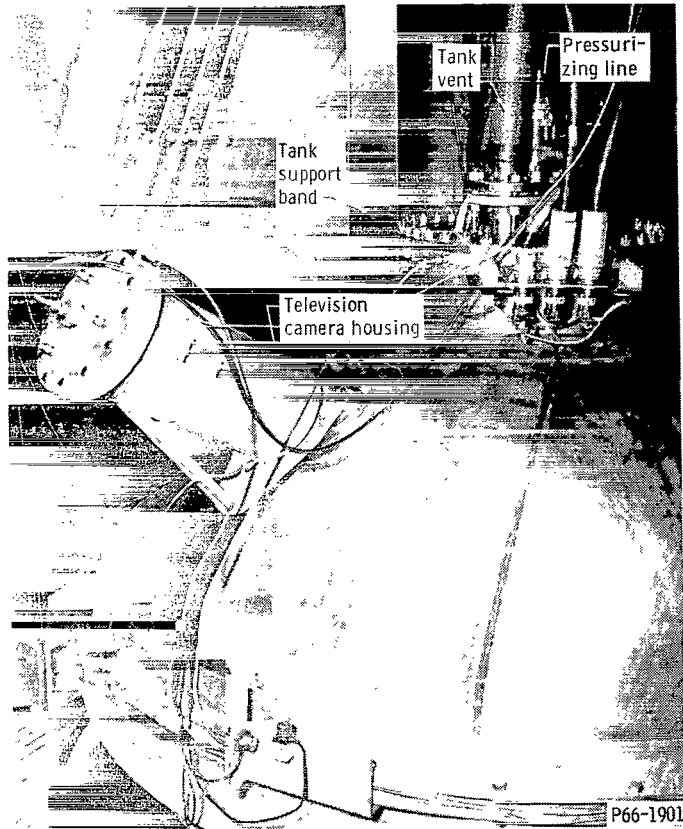
Figure 4. - View port and television camera installation on test tank. Wall thickness, 0.762 centimeter (0.30 in.).


→ Denotes pressurant gas flow paths
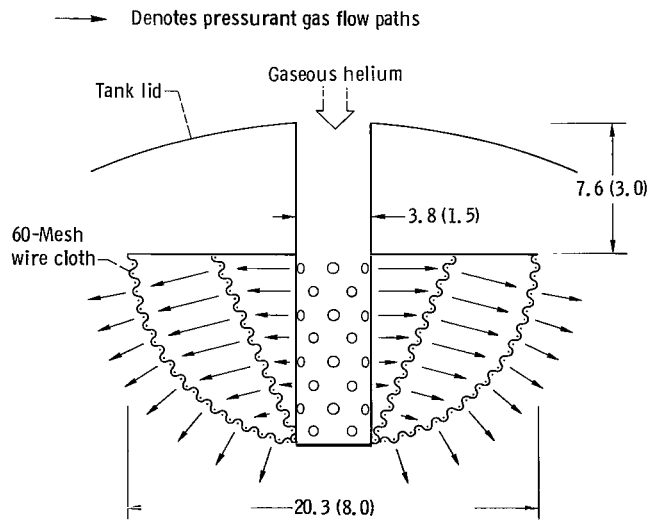
Figure 5. - Injector geometry for hemisphere injector.
Open area, 176.8 square centimeters (27.4 in.^{2}).
All dimensions are in centimeters (in.).

11

Internal Tank Instrumentation

Temperatures. - Ullage gas temperatures together with gas concentration measurements were used to determine the mass and energy content of the tank ullage. The temperatures must be obtained with sensors capable of accurate measurement of rapid changes in temperature. Internal tank instrumentation is illustrated in figure 6. Location of the vertical and horizontal ullage gas temperature rakes is indicated. The thermopile was the basic temperature measurement technique used in this investigation. The use of thermopiles to measure ullage gas temperature was first developed in reference 6, and the technique was used with good results in references 3 to 5. The main advantage of using thermopiles is their fast response time (between 0.2 and 1.0 sec) in going from saturated liquid to vapor. This time response is approximately an order of magnitude less than carbon or platinum resistance sensors which are generally used in this type of investigation.

A typical three-element thermopile unit and its associated wiring schematic are illustrated in figure 7. The thermopile units were constructed of 0.202 millimeter (0.008 in.) chromel-constantan wire. Vertical ullage gas temperature profiles were obtained by stacking the individual thermopile units as shown in figure 7(b). The support structure was made of laminated thermoplastic to minimize thermal conduction from one measure-
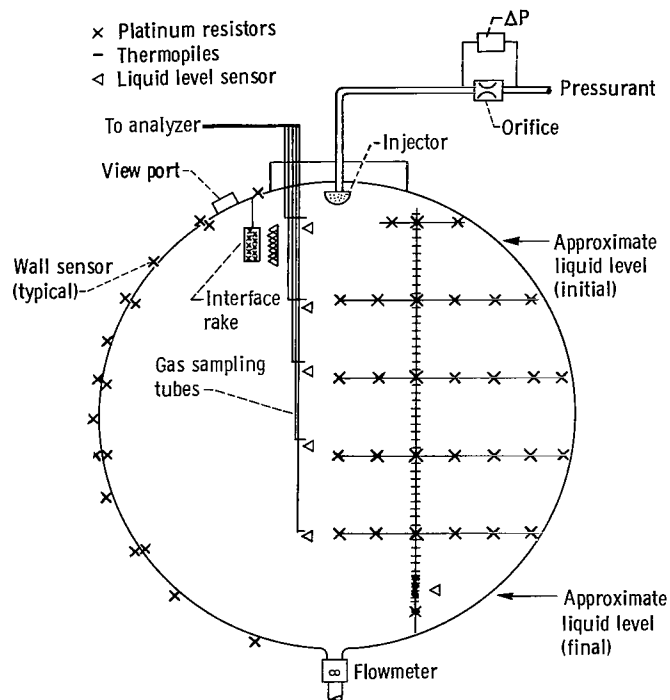

Figure 6. - Test tank instrumentation.
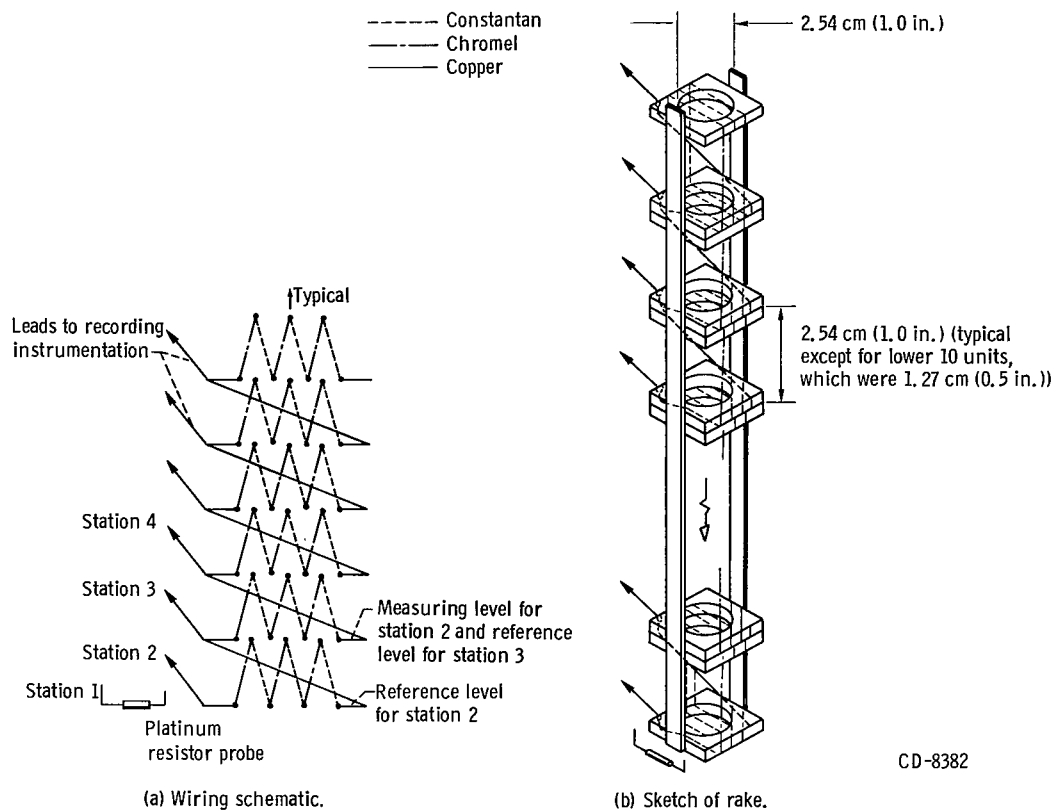
Figure 7. - Thermopile rake.

ment station to another. The spacing between the reference and measuring levels was 2.54 centimeters (1.0 in.) for the top 45 thermopiles composing the vertical rake. The 10 units at the bottom of the rake had spacings of 1.27 centimeters (0.50 in.) to obtain a more accurate temperature profile of the ullage gas near the liquid surface at the end of an expulsion.

Platinum resistance sensors, which were located at least every tenth station starting from the bottom of the rake, sensed the absolute temperature at their location and provided a reference for the thermopiles above the location.

The horizontal rakes were composed of platinum resistance sensors spaced a maximum of 12.70 centimeters (5.00 in.) apart in the radial direction. Two platinum resistance sensors were used at each location to measure liquid and/or gas temperatures for the ranges of 20 to 38.9 K (36° to 70° R) and 38.9 to 277.8 K (70° to 500° R). These dual sensors permitted more accurate measurement of liquid and gas temperatures than could be achieved with one sensor covering the entire range.

The initial static temperature profile near the liquid surface was determined by a fixed interface rake. This rake contained 13 platinum resistance sensors spaced 0.64

13

centimeter (0.25 in.) apart. The range of these sensors was 20 to 38.9 K (36° to 70° R). For complete tank expulsions (i.e., 5 percent ullage to 5 percent outage), the initial liquid level was always assured to be on the interface rake in the thick walled tank by monitoring a closed-circuit television system which viewed, through a viewport in the tank, the position of the liquid-gas interface on a scale fixed to the interface rake (fig. 6). For tests conducted at the 28-, 55-, and 75-percent ullage values, the scale was moved lower in the tank and the television camera was refocused. Liquid level for the thin walled tank was determined by hot-wire liquid level sensors located on the interface rake.

Platinum resistance sensors were also used to determine tank wall temperatures at 12 locations and the liquid temperature at the flowmeter. Copper-constantan thermocouples were used to determine tank lid temperatures at 5 locations and the pressurant gas inlet temperature.

Concentrations. - The concentration of helium and hydrogen gas at five positions in the tank (fig. 6) was obtained by a gas sampling and analyzer system. A general schematic of this system is shown in figure 8. The sampling tubes had a 0.157-centimeter (0.062-in.) outside diameter with a wall thickness of 0.030 centimeter (0.012 in.). The analyzing sequencing of the five sampling tubes was done automatically. The sampling operation for one tube was as follows: The sample tube was purged with a negligible flow of helium until the liquid surface passed the entrance of the tube at which time it was included in the sampling sequence of the tubes above it. The gas sample was vented (also
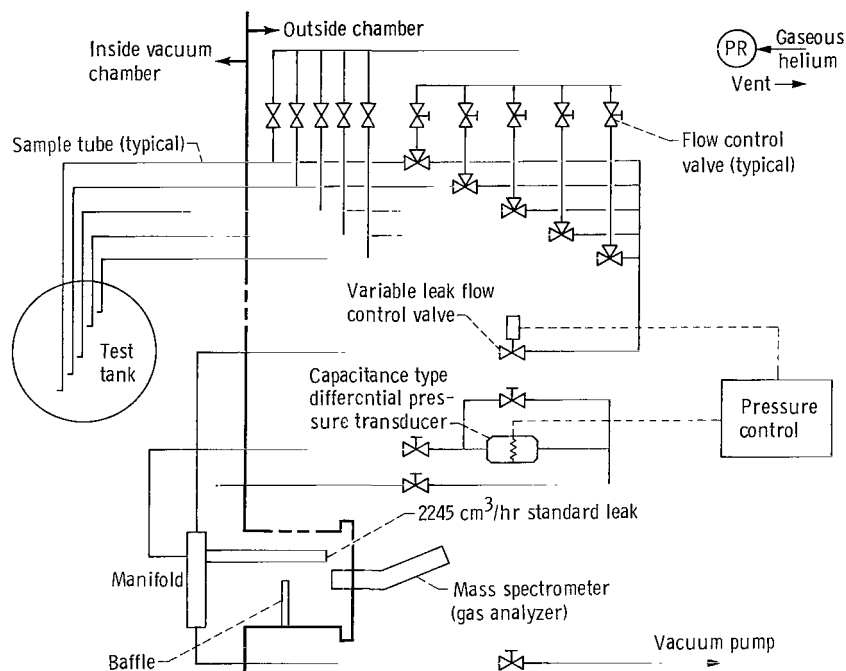

Figure 8. - Schematic of gas analyzer system.

at a negligible rate) to the atmosphere until its particular level was to be analyzed. At this time the flow control vent valve was closed and the sample flow was directed through a variable-leak flow control valve to a constant pressure manifold from where a portion of the sample passed through a 2245 cubic centimeter per hour standard leak to a mass spectrometer. The mass spectrometer then measured the partial pressure of the hydrogen of the gas sample which was used to determine the hydrogen concentration at that level. The manifold and tube were then evacuated and the next level in the sequence was sampled and analyzed. The total time required to sample and analyze each level was approximately 8 seconds.

All measurements except the gas concentrations were recorded on a high-speed digital data system. The measurements were recorded at a rate of 3.125×10^3 channels per second. Each measurement channel was sampled every 0.064 second. The gas concentration measurements were continuously recorded on a direct reading oscillograph.

PROCEDURE

The spherical test tank was filled from the bottom to approximately a 2-percent ullage condition. It was then topped off as necessary while the tank lid and peripheral support hardware reached steady-state operating temperatures.

Temperature conditioning of the pressurant gas was then started. Gas flow was established through the heat exchanger loop, through the control valves and orifice arrangement, and then into the tank ullage from where it was vented through the conditioning line to the outside as shown in figure 2. The temperature control circuit shown in figure 2 was used to get the desired pressurant gas temperature level during the flow period. When the pressurant gas temperature conditioning was almost completed, the liquid level in the test tank was adjusted to a desired value by either topping or slow draining.

The pressurant gas flow was then stopped and the test tank was vented in preparation for an expulsion run. The automatic controllers and timers were preset with all the desired run and operating conditions (i.e., tank pressure level, length of ramp period, length of hold period, liquid outflow valve position, start and stop times of the data recording equipment, etc.).

After starting the data recording equipment, the next step of the completely automatic run sequence took electrical calibrations on all pressure transducers. Immediately following this, the test tank was pressurized over a predetermined time period to the nominal operating pressure of 34.47×10^4 newtons per square meter (50 psia). Tank pressure was held constant for about 30 seconds to stabilize internal temperatures. The tank expulsion period was then started. Approximately 90 percent of the total tank volume was expelled at a constant volumetric flow rate. The expulsion period was stopped

when a hot-wire liquid level sensor located at the 95-percent ullage level indicated the presence of gas. The last step of the automatic run sequence was the stopping of all data recording equipment. The test tank was then vented and refilled with liquid hydrogen for the next expulsion.

Additional ramp pressurization runs, with no expulsion, were made for three different tank ullage levels.

DATA REDUCTION

The data reduction procedure used in this report is essentially the same that was used in reference 4 with the exception of the treatment for the two component ullage. The complete data reduction procedure is presented in appendix D. The relations derived in appendix D that are used in the presentation of experimental results are now summarized.

Pressurant Gas Added (M_G)

The actual pressurant added to the tank ullage was determined from the relation

$$M_{G, i \to f} = \int_{t_i}^{t_f} YD^2C \sqrt{\rho \Delta P^*} \, dt \tag{1}$$

Ideal Pressurant Requirement (M_I)

This report uses two different relations to define the ideal pressurant requirement. One is used to determine the ideal requirement for the initial pressurization of the tank and is given by

$$M_I = \frac{\overline{M} P_o V_o}{ZRT_G} \left[\left(\frac{P_f}{P_o} \right)^{1/\gamma} - 1 \right] \tag{2}$$

This expression assumes a one component ullage. It also assumes that the pressurizing gas does not mix or exchange heat with the gas in the ullage volume. For the tests conducted herein, the initial ullage volume contained a mixture of hydrogen and helium. However, because of the method used to precondition the inlet gas temperature (described in the PROCEDURE section), the initial ullage volume was predominantly helium.

16

Therefore, the ideal pressurant requirement used in this report is based on a 100-percent helium ullage (i.e., $\overline{M} = 4.003$, $\gamma = 1.67$), whereas the ideal requirement used in reference 4 is based on 100-percent hydrogen (i.e., $\overline{M} = 2.016$, $\gamma = 1.40$). In any case, the ideal requirement is just used as a normalizing factor and does not necessarily indicate a true minimum requirement.

The other relation, which is used to determine the ideal requirement during the expulsion period, is given by

$$M_i = \frac{\overline{M}P \, \Delta V_U}{ZRT_G} \tag{3}$$

The assumption used to obtain this relation is that the incoming pressurant does not exchange heat or mass with the surroundings.

Energy Balance

Applying the first law of thermodynamics to the entire tank system (tank + ullage gas + liquid) results in the expression

$$\underbrace{\int_{t_i}^{t_f} (\dot{M}_G h_G + \dot{Q}) dt}_{\substack{\text{Total energy} \\ \text{added} \\ (\Delta U_T)}} = \underbrace{\int_{t_i}^{t_f} (\dot{M}_L h_L \, dt + dU_L)}_{\substack{\text{Total change in liquid} \\ \text{in tank + liquid} \\ \text{expelled energy} \\ (\Delta U_L)}} + \underbrace{\int_{t_i}^{t_f} dU_U}_{\substack{\text{Total change} \\ \text{in ullage} \\ \text{energy} \\ (\Delta U_U)}} + \underbrace{\int_{t_i}^{t_f} dU_w}_{\substack{\text{Total change} \\ \text{in wall} \\ \text{energy} \\ (\Delta U_w)}} \tag{4}$$

Dividing equation (4) by ΔU_T gives

$$1 = \frac{\Delta U_L}{\Delta U_T} + \frac{\Delta U_U}{\Delta U_T} + \frac{\Delta U_w}{\Delta U_T} \tag{5}$$

These ratios show the relative distribution of the total energy input into the system. The data for energy distribution presented herein are in the form of these ratios.

TABLE I. - MASS BALANCE RESULTS FOR HEMISPHERE INJECTOR

[Tank pressure, 34.47×10^4 N/m^2.]

Run	Tank wall thickness, cm	Inlet gas temperature K	°R	Ramp time, sec	Hold time, sec	Expulsion time, sec	Tank cycle time, sec	Ramp Initial ullage mass, kg	Mass added during ramp, kg	Mass transfer during ramp, kg	Hold Ullage mass after ramp, kg	Mass added during hold, kg	Mass transfer during hold, kg	Ullage mass after hold, kg	Expulsion Mass added during expulsion, kg Experimental (a)	Predicted	Mass transfer during expulsion, kg	Final ullage mass, kg
83	0.762	263	473	15.6	22.2	391.0	428.8	0.093	0.063	0.038	0.118	0.053	0.020	0.151	3.199±0.001	3.557	-0.176	3.526
84		266	479	15.7	21.6	267.3	304.6	.101	.072	.036	.137	.058	.016	.178	2.978±0.001	3.098	.140	3.016
85		271	488	16.0	21.6	136.8	174.4	.108	.073	.044	.138	.062	.006	.194	2.472±0.002	2.508	.457	2.209
88		184	331	14.6	22.1	396.2	432.8	.082	.073	-.027	.182	.062	.064	.179	3.483±0.002	4.159	.324	3.338
92		170	306	14.5	22.3	138.0	174.8	.108	.068	-.036	.213	.050	.078	.184	2.969±0.002	3.188	.159	2.994
94		324	583	15.9	20.5	395.4	431.8	.090	.054	.028	.117	.064	.022	.158	3.024±0.001	3.439	-.213	3.395
95		311	560	15.7	20.8	271.2	307.6	.087	.050	.020	.117	.055	.017	.156	2.779±0.002	2.834	-.071	3.006
97		335	603	16.6	20.0	133.9	170.5	.101	.064	.023	.142	.066	.034	.173	2.235±0.001	2.175	.136	2.272
7	0.409	287	517	25.2	27.4	400.9	453.4	0.091	0.079	0.059	0.111	0.039	-0.020	0.170	2.893±0.001	3.147	-0.039	3.102
10		292	526	25.1	27.6	140.5	193.2	.086	.073	.051	.108	.033	-.022	.164	2.315±0.001	2.319	.116	2.363
12		285	513	24.9	27.4	340.9	393.2	.085	.071	.047	.109	.037	-.010	.156	2.860±0.001	2.927	.069	2.947
14		288	518	24.5	28.4	284.2	337.0	.084	.068	.029	.124	.032	.008	.148	2.760±0.001	2.805	.139	2.769
15		291	524	24.8	27.7	197.2	249.7	.087	.068	.041	.114	.034	-.013	.161	2.514±0.001	2.556	.159	2.516

[a] ±Value is probable error associated with each measurement.

TABLE II. - ENERGY BALANCE RESULTS

Run	Tank wall thick- ness, cm	Inlet gas temper- ature K	°R	Expul- sion time, sec	Energy added by pressurant gas, J Experimental (a)	Predicted	Energy added by environ- ment, J	Energy gained by tank wall, ΔU_W, J Experimental	Predicted	Energy gained by ullage, ΔU_U, J	Energy gained by liquid, ΔU_L, J Experimental (a)	Predicted
83	0.762	263	473	391.0	$442.6\pm0.2\times10^4$	488.0×10^4	28.6×10^4	256.5×10^4	259.0×10^4	105.2×10^4	$94.4\pm43.3\times10^4$	98.3×10^4
84		266	479	267.3	414.8±0.2	431.0	19.6	228.3	232.8	118.8	93.7±36.8	67.8
85		271	488	136.8	350.2±0.2	355.7	9.9	179.9	175.7	112.5	46.7±21.4	34.7
88		184	331	396.2	345.5±0.2	401.9	29.0	175.1	174.8	157.0	77.0±44.5	99.7
92		170	306	138.0	278.1±0.2	296.3	10.1	108.7	106.4	125.0	86.6±19.9	34.8
94		324	583	395.4	529.0±0.2	593.6	29.0	313.5	354.9	117.3	99.2±39.0	130.0
95		311	560	271.2	502.1±0.3	511.1	19.7	292.0	312.7	117.2	66.8±34.6	68.2
97		335	603	133.9	411.3±0.2	401.6	9.8	204.7	227.8	100.3	142.0±14.3	33.8
7	0.409	287	517	400.9	$433.1\pm0.2\times10^4$	466.9×10^4	30.0×10^4	241.2×10^4	254.9×10^4	115.1×10^4	$85.6\pm28.8\times10^4$	105.6×10^4
10		292	526	140.5	355.5±0.1	356.6	10.3	171.2	157.0	109.4	89.7±28.6	36.7
12		285	513	340.9	428.7±0.1	437.9	24.9	233.8	220.9	113.1	93.1±27.6	89.1
14		288	518	284.2	417.1±0.1	423.3	20.8	223.1	210.4	114.5	119.1±27.5	74.9
15		291	524	197.2	381.1±0.1	380.9	14.4	195.1	188.2	112.3	86.9±22.9	51.8

a ±Values is probable error associated with each measurement (absolute value).

Error Analysis

An analysis was performed to determine the magnitude of probable error which could be present in the integrations of equations (D4), (D13), and (D14). Probable error is defined as follows: There is a 50-percent probability that the error will be no larger than the value stated. This analysis considered the errors introduced by the inaccuracies of temperature transducers as well as the tank pressure sensor. These calculations were performed for all runs for the expulsion period. The results of this analysis are included with the tabular expulsion data in tables I and II. No error analysis was performed on parameters which were dependent on the measured gas concentration data. The actual uncertainty of determining the gas concentration was unknown although it was estimated to be between ±10 to ±30 percent.

RESULTS AND DISCUSSION

The main parameter used to compare the effectiveness of the various operating parameters on the amount of pressurant gas used is the nondimensional ratio M_I/M_G. The symbol M_I is defined as the ideal helium pressurant mass required to pressurize or expel a given volume of liquid at a given inlet gas temperature and tank pressure assuming no heat or mass transfer, and M_G is the actual pressurant requirement for the same inlet gas temperature and tank pressure. A high M_I/M_G ratio means less energy and mass exchange. It does not necessarily mean a lower absolute pressurant requirement M_G as will be illustrated later in this section.

A value of M_I/M_G equal to 1 implies that there is no heat transferred to the tank wall or liquid and no mass transfer. This means that for no environmental heating the terms $\Delta U_w/\Delta U_T$ and $\Delta U_L/\Delta U_T$ in equation (5) of the DATA REDUCTION section are zero and that $\Delta U_U/\Delta U_T$ is equal to 1; that is, all the energy (ΔU_T) added to the tank during expulsion appears as an increase in ullage energy (ΔU_U). Therefore, any value of M_I/M_G or $\Delta U_U/\Delta U_T$ less than 1 means energy is lost by the ullage system. This loss of ullage energy would then appear as a change in tank wall energy and/or liquid energy; that is, $\Delta U_w/\Delta U_T$ and/or $\Delta U_L/\Delta U_T$ would be greater than zero.

The discussion of results first presents the effects of the various operating parameters on the ratio M_I/M_G for the expulsion period only, which was of primary interest, followed by the mass transfer M_t/M_G results. Then the results of the energy balances are presented in an attempt to point out major reasons for the ratios M_I/M_G or $\Delta U_U/\Delta U_T$ being less than 1. Finally, a comparison is made between the experimental results and the analytically predicted results to determine the validity of the analytical program. The analytical results are presented in the figures along with the correspond-
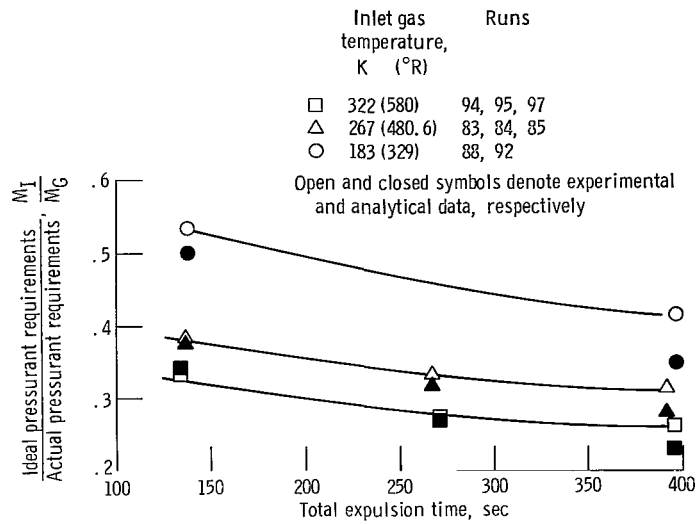
Figure 9. - Comparison of ideal pressurant requirement to actual pressurant requirement ratio as function of expulsion time for three inlet gas temperatures. Tank pressure, 34.47×10^4 newtons per square meter (50 psia); wall thickness, 0.762 centimeter (0.30 in.).

ing experimental results. The comparison between experimental and analytical results are given in terms of an average deviation, which is defined as

$$\frac{1}{\overline{N}} \sum_{\overline{N}} \left[\frac{|(\text{Experimental ratio}) - (\text{Analytical ratio})|}{(\text{Experimental ratio})} \right] (100) \qquad (27)$$

where $\overline{N}$ is the number of data points in a given set of operating conditions (i.e., for a constant inlet gas temperature of 322 K (580° R), $\overline{N}$ would be 3 for the data presented in fig. 9). For convenience, all deviations between the experimental and analytical results are summarized in table III.

The operating parameters (e.g., inlet gas temperature, outflow rate, and tank wall thickness) and major experimental and analytical results are summarized in tables I and II. Table I gives the experimental and analytical mass balance results, while table II gives the corresponding energy balance results.

Effect of Inlet Gas Temperature

Pressurant requirements. - The effect of inlet gas temperature is shown in figure 9 on the basis of M_I/M_G for various expulsion times. Expulsion time is the total time

TABLE III. - DEVIATIONS BETWEEN EXPERIMENTAL AND ANALYTICAL

RESULTS FOR HEMISPHERE INJECTORS

Run	Inlet gas temperature		Tank wall thickness, cm	Percent deviation between experimental and analytical results[a]		
	K	^{O}R		M_I/M_G	$\Delta U_W/\Delta U_T$	$\Delta U_L/\Delta U_T$
83	263	473	0.762	+10.25	-0.91	-4.00
84	266	479		+3.92	-2.09	+27.77
85	271	488		+1.57	+2.20	+26.15
88	184	331		+16.38	0	-29.12
92	170	306		+6.54	+2.11	+59.80
94	324	583		+12.21	-13.16	-30.89
95	311	560		+1.79	-7.15	-2.34
97	335	603		-2.40	-11.31	+76.26
7	287	517	0.409	+7.82	-5.75	-23.24
10	292	526		+.25	+8.33	+59.18
12	285	513		+2.14	+5.43	+4.39
14	288	518		+1.48	+5.88	+37.13
15	291	524		+.84	+3.60	+40.36

[a]Analysis overpredicts, -; analysis underpredicts, +.

required to expel liquid from a 5-percent ullage to a 95-percent ullage. Therefore, each data point represents a complete expulsion. For a given inlet gas temperature, there is an increasing pressurant requirement (decreasing M_I/M_G) for increasing expulsion times. The longer the pressurant (ullage) gas is exposed to the cold surroundings, the greater the loss in pressurant energy. The ratio M_I/M_G also decreases for increasing inlet gas temperature (from 0.540 for the 183 K (329° R) inlet gas temperature at a 138-second expulsion to 0.263 for the 322 K (580° R) inlet gas temperature at a 395-second expulsion). This decreasing ratio implies that a larger percentage of the pressurant gas energy is lost to the tank wall and/or to the liquid as the inlet gas temperature is increased. The values of M_I/M_G obtained here using helium as the pressurant are approximately the same as those obtained in reference 4 using hydrogen as the pressurant for similar inlet gas temperatures and expulsion times. A comparison of the actual pressurant requirements M_G for the three inlet gas temperatures for various expulsion times is shown in figure 10. The actual pressurant requirements (M_G) decrease for increasing inlet gas temperature and increase for increasing expulsion times. There is an average decrease of 1.3 percent in M_G for a 10 K (18° R) increase in inlet gas temperature. The results of reference 4 indicated that there was an average decrease in pressurant gas requirements of 1.4 percent for a 10 K (18° R) increase in inlet gas temperature when using hydrogen as the pressurant gas.
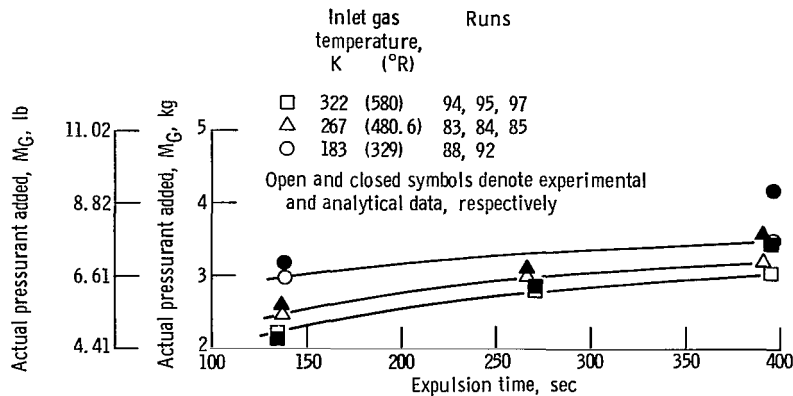
Figure 10. - Comparison of actual pressurant added as function of expulsion time for three inlet gas temperatures. Tank pressure, 34.47×10^4 newtons per square meter (50 psia); wall thickness, 0.762 centimeter (0.30 in.).

Although the absolute value of M_G decreases for increasing inlet gas temperatures, the ratio M_I/M_G at 322 K (580° R) is less than the M_I/M_G ratio at 183 K (329° R) because of the greater decrease in ideal requirements.

The shaded symbols shown in figures 9 and 10 are the results as predicted by the analytical program. The agreement between the analysis and experimental results is better for the 322 and 267 K (580° and 480.6° R) inlet gas temperatures (see table III for actual deviations) than for the 183 K (329° R) inlet temperature. The reason for the greater deviation for the lower temperature is not clearly understood. The deviation between the analytical and experimental results is also greatest for the longest expulsion time in all cases. This could be attributed to the diffusion of hydrogen into the helium ullage (to satisfy its partial pressure) which is a time-dependent process. The longer the liquid hydrogen is exposed to a helium ullage the more hydrogen will diffuse into the ullage. The limiting condition is when the partial pressure of hydrogen in the ullage is satisfied. The addition of hydrogen into the ullage would therefore reduce the actual helium pressurant requirement. The analysis does not consider this mass transfer and would therefore overpredict the pressurant requirements, especially for the longer expulsion times.

Mass transfer. - The amount of mass transfer was not directly measured experimentally. It was determined indirectly by the use of equation (D8). The accuracy of determining the mass transfer is strongly influenced by the accuracy in which the gas sampling and analysis system determines the helium-hydrogen concentrations in the ullage.

A comparison of the ratio of mass transferred during expulsion to the actual pressurant added to the tank M_t/M_G is presented in figure 11 for different expulsion times and the three inlet gas temperatures. The experimental results presented in this figure indicate that helium is absorbed into the liquid hydrogen for the short expulsion times for

23

Inlet gas   Runs
temperature,
K (°R)

□   322 (580)   94, 95, 97
△   267 (480.6)   83, 84, 85
○   183 (329)   88, 92

Evaporation

Absorption/
Condensation

Mass transfer
Actual pressurant added' $\frac{M_t}{M_G}$

.2

0

.2
100   150   200   250   300   350   400
Expulsion time, sec
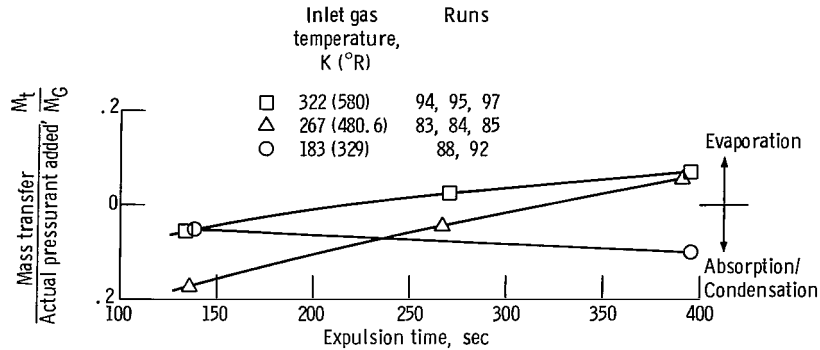
Figure 11. - Comparison of mass transfer to mass added ratio as function of expulsion time for three inlet gas temperatures. Tank pressure, 34.47x10⁴ newtons per square meter (50 psia); wall thickness, 0.762 centimeter (0.30 in.).

the three inlet gas temperatures. Both the 322 and 267 K (580° and 480.6^O R) inlet gas temperatures show a trend toward evaporation of liquid for increased expulsion times. This trend is not apparent for the 183 K (329° R) inlet gas temperature.

As mentioned previously, the determination of mass transfer is strongly influenced by the determination of the helium-hydrogen gas concentration in the ullage. Figure 12 compares the ullage gas concentration profiles prior to and after expulsion for a run which indicated absorption (run 85) and a run which indicated evaporation (run 83). Both runs show an increase of hydrogen gas in the ullage over the expulsion period. This fact alone indicates evaporation and/or diffusion. However, the percent of helium near the liquid surface (where most of the ullage mass is concentrated) for run 85 was much less than that of run 83, resulting in a much lower final ullage mass. The use of equation (8) (appendix D) for run 85 results in a value of mass transfer (absorption) of 0.458 kilogram (1.009 lb). Based on a 1.2-mole-percent solubility of helium in liquid hydrogen (ref. 7) the maximum amount of helium that could go into solution is approximately 2.618 kilogram (5.770 lb). Even though all absorption values were well below this maximum value, the actual mass-transfer values are considered inconclusive because of the rather large uncertainties in determining concentration gradients.

There are no analytical comparisons for the mass transfer because the analysis neglects mass transfer in its development.

Energy remaining in ullage. - The ratios of the energy increase in the ullage over the expulsion period to the total energy added to the system $\Delta U_U / \Delta U_T$ for different expulsion times are compared in figure 13 for the three inlet gas temperatures. For all runs, between 21.0 and 43.5 percent of the total energy that was added to the system remains in the ullage after expulsion. In general, the ratio $\Delta U_U / \Delta U_T$ decreases for increasing inlet gas temperatures for a constant expulsion time. Also, for a given inlet gas temperature, the ratio $\Delta U_U / \Delta U_T$ decreases with increasing expulsion time. It should be noted that the absolute value of ΔU_U does not change significantly for the
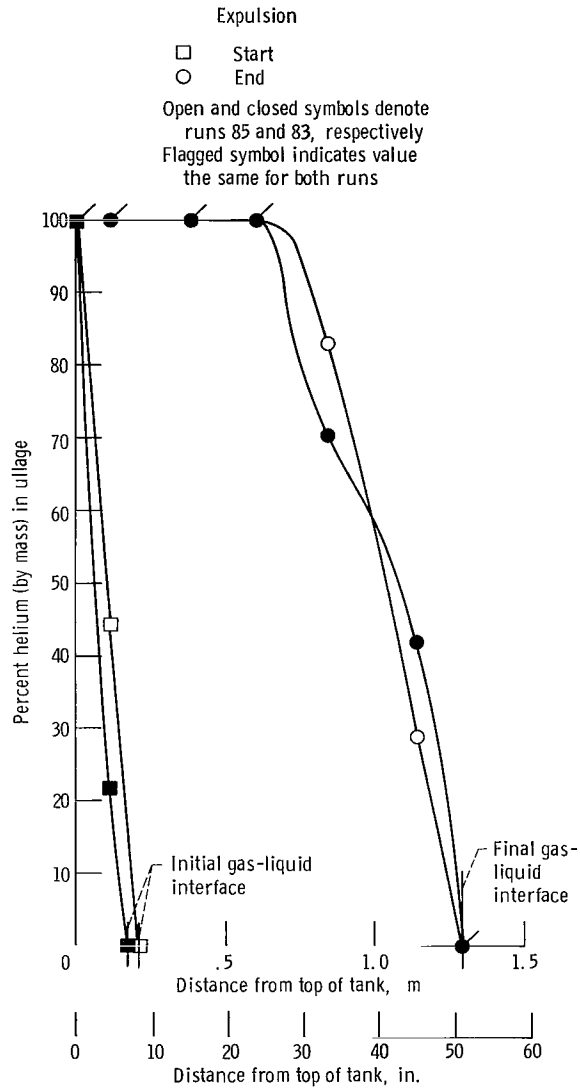
Figure 12. - Comparison of ullage gas concentration
profiles prior to and after expulsion for runs 83,
which indicated evaporation, and 85, which indicated
absorption. Tank pressure, 34.47x10⁴ newtons per
square meter (50 psia); inlet gas temperature: for
run 85, 271 K (488° R); for run 83, 263 K (473° R).
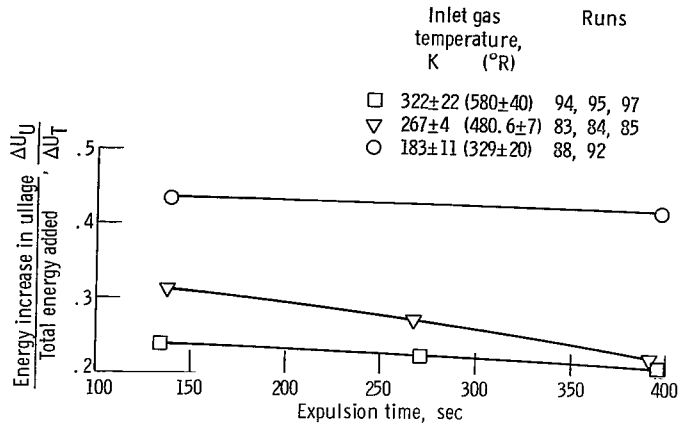
Figure 13. - Comparison of energy increase in ullage to total energy added ratio as function of expulsion time for three inlet gas temperatures. Tank pressure, 34.47×10^4 newtons per square meter (50 psia); wall thickness, 0.762 centimeter (0.30 in.).

three operating inlet gas temperatures used during testing. The mean increase in ullage energy for these series of runs (table II) was 117×10^4 joules (1106 Btu) with a standard deviation of 13.7×10^4 joules (129 Btu). Any trends in the ratio $\Delta U_U / \Delta U_T$, therefore, depend mainly on variations in the total energy added (ΔU_T) to the system due to variations in energy losses to the tank wall and liquid.

Energy added to tank wall. - The ratios of energy gained by the tank wall to the total energy added to the system $\Delta U_W / \Delta U_T$ for different expulsion times are compared in figure 14 for the three inlet gas temperatures. In general, between 37.5 and 56.2 per-
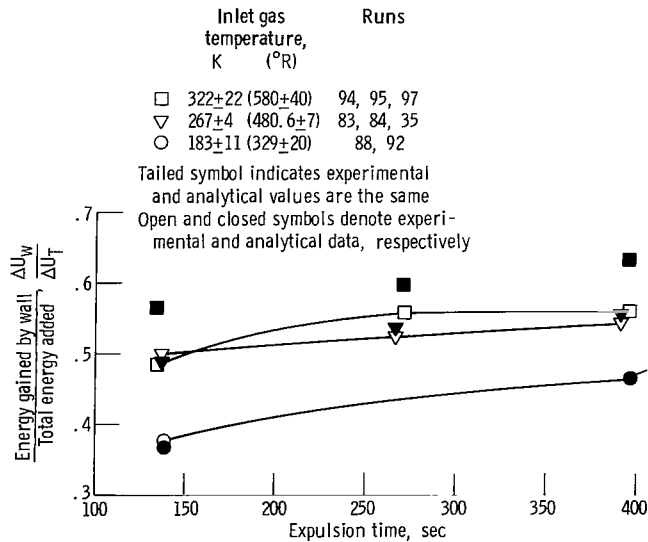

Figure 14. - Comparison of energy gained by wall to total energy added ratio as function of expulsion time for three inlet gas temperatures. Tank pressure, 34.47×10^4 newtons per square meter (50 psia); wall thickness, 0.762 centimeter (0.30 in.). Curves are faired through experimental data.

cent of the total energy added to the system was gained by the tank wall over the range of conditions. The results of reference 4 showed that between 30 and 58.8 percent of the total energy added to the tank was gained by the tank wall for similar test conditions when using hydrogen as the pressurant. A comparison of results indicate that there is generally a 5 to 7.5 percent increase in the percent of total energy that is lost to the tank wall when using helium as the pressurant. As can be seen in table II and in figure 14, both the absolute value of ΔU_w and the ratio $\Delta U_w/\Delta U_T$ increase with increasing inlet gas temperature. The increase in ΔU_w is due to the larger driving potential ΔT for heat transfer between the ullage gas and the tank wall. The total energy added to the system (ΔU_T) does not increase in the same proportion as ΔU_w resulting in the increased ratio $\Delta U_w/\Delta U_T$.

The agreement between the analysis and experimental value of $\Delta U_w/\Delta U_T$ are very good for the 183 and 267 K (329° and 480.6^O R) inlet gas temperature (within ±2.2 percent, see table III). However, the agreement for the 322 K (580° R) inlet gas is not as good (within ±13.2 percent).

Energy gained by liquid. - Figure 15 is a comparison of the ratio of energy gained by the liquid to the total energy added to the system $\Delta U_L/\Delta U_T$ for different expulsion times for the three inlet gas temperatures. In all cases, between 12.8 and 33.7 percent of the total energy added to the system appears as an increase in liquid energy (liquid heating). The results of reference 4 indicated that between 15 and 25 percent of the total energy added to the system appears as an increase in liquid energy for similar test conditions using hydrogen as the pressurant. There is a relatively large amount of scatter
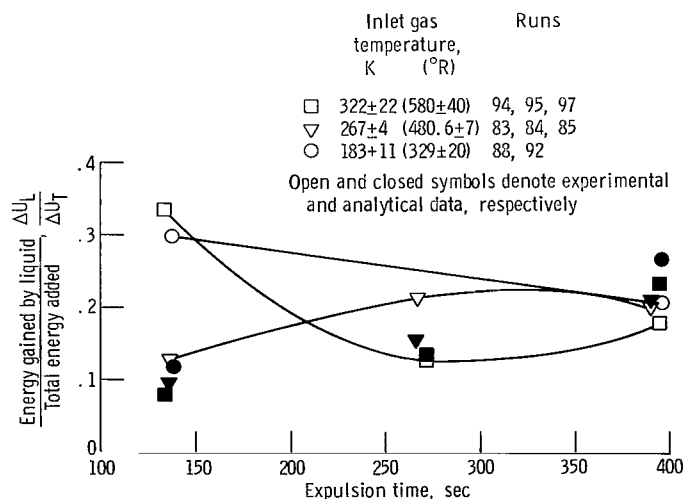
Figure 15. – Comparison of energy gained by liquid to total energy added ratio as function of expulsion time for three inlet gas temperatures. Tank pressure, 34.47×10^4 newtons per square meter (50 psia); wall thickness, 0.762 centimeter (0.30 in.). Curves are faired through experimental data.

in the data shown in figure 15. This scatter could be the result of the error in experimentally determining ΔU_L. The probable error associated with each experimental determination of ΔU_L is between 10 and 58 percent (i.e., 14.3×10^4 out of 142.0×10^4 J and 44.5×10^4 out of 77.0×10^4 J, see table II).

The analytical predictions of the ratio $\Delta U_L / \Delta U_T$ are also presented in figure 15 (see table III for average deviations). The large discrepancy between the analysis and experimental results could also be the result of the error in determining ΔU_L.

Temperature distributions. - The results that were discussed previously point out that between 72.4 and 88.6 percent of the total energy that was added to the system is either absorbed by the tank wall or remains in the ullage. The correlation between the analysis and experimental data, therefore, depends largely on the ability of the analysis to predict final wall and ullage gas temperature profiles. These profiles are, in turn, used to determine the increase in wall and ullage energy and the final ullage mass. The ability to predict these temperatures explains the fair agreement between experimental data and analysis reported in references 1 and 3 to 5.

Figure 16 presents comparisons of experimental and analytical ullage gas and wall temperature profiles for the three inlet gas temperatures. Figure 16(a) presents a comparison of experimental and analytical wall and ullage gas temperature profiles at the end of a 396-second expulsion for an inlet gas temperature of 184 K (331° R). For this run the analysis accurately predicted the $\Delta U_w / \Delta U_T$ ratio but underpredicted the M_I / M_G ratio by 16.38 percent. The experimental gas temperatures shown in figure 16(a) were obtained from the vertical rake. The horizontal rakes indicate these are average radial temperatures at their respective vertical position. In the absence of any mass transfer, the pressurant mass required for an expulsion could be determined as the difference between the final mass in the ullage and the initial mass prior to expulsion.

One of the inputs to the analytical program is the initial experimental temperature profile prior to expulsion. The analytical program uses this profile together with the temperature-density relation for helium to obtain the initial ullage mass. The initial ullage mass as determined by the analysis is, in all cases, larger than determined experimentally because the experimental values contain hydrogen in the ullage. However, the difference between the analytically and experimentally determined initial ullage mass represents only a small fraction (less than 3 percent) of the final ullage mass. Therefore, the deviation between the analytical and experimental pressurant requirements would largely be the result of the predicted final ullage temperature profile. As seen in figure 16(a) the analytical gas temperatures are slightly lower in the lower 20 percent of the tank but begin to get higher toward the top of the tank. The overprediction of temperatures in the majority of the ullage results in a 16.38-percent underprediction in the final ullage mass.

The analytically predicted wall temperatures (fig. 16(a)) are very close to those ob-
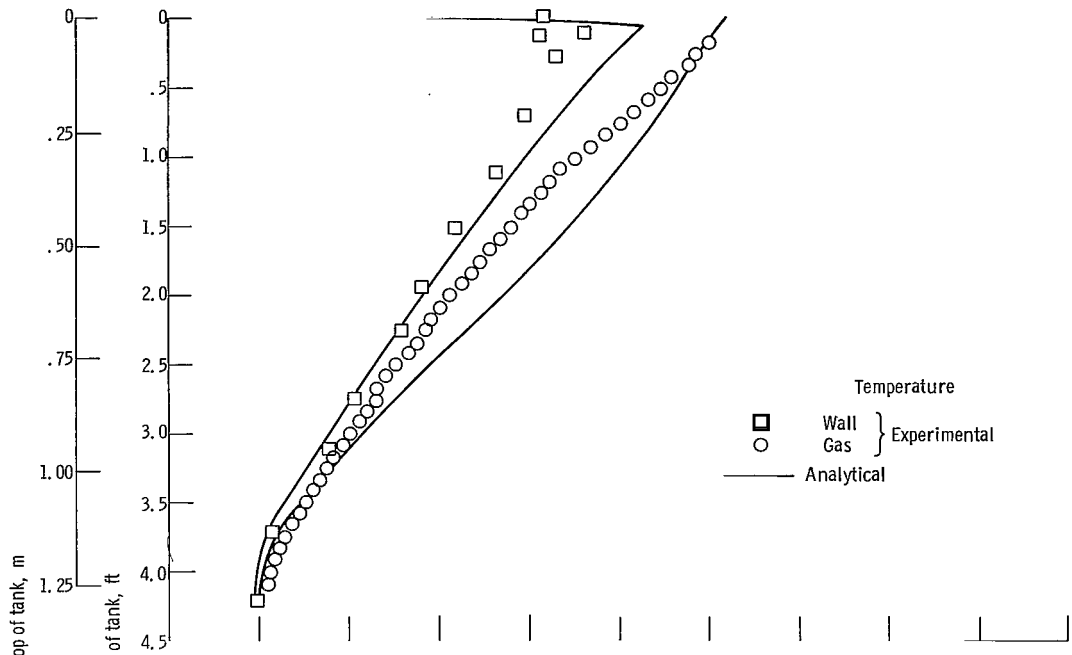
(a) Expulsion time, 396 seconds; inlet gas temperature, 184 K (331° R); run 88.

Temperature
□ Wall   } Experimental
○ Gas   }
—— Analytical
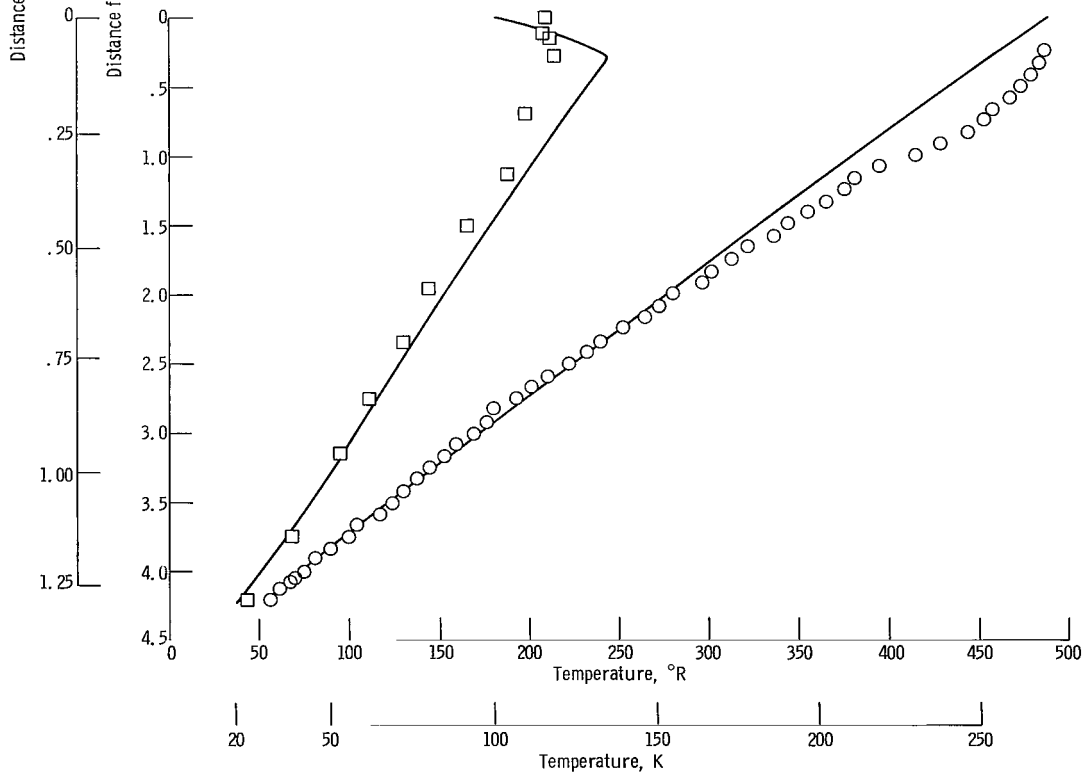
(b) Expulsion time, 137 seconds; inlet gas temperature, 271 K (488° R); run 85.

Figure 16. – Comparison of analytical and experimental gas and wall temperatures. Tank pressure, 34.47x10^4 newtons per square meter (50 psia); wall thickness, 0.762 centimeter (0.30 in.).
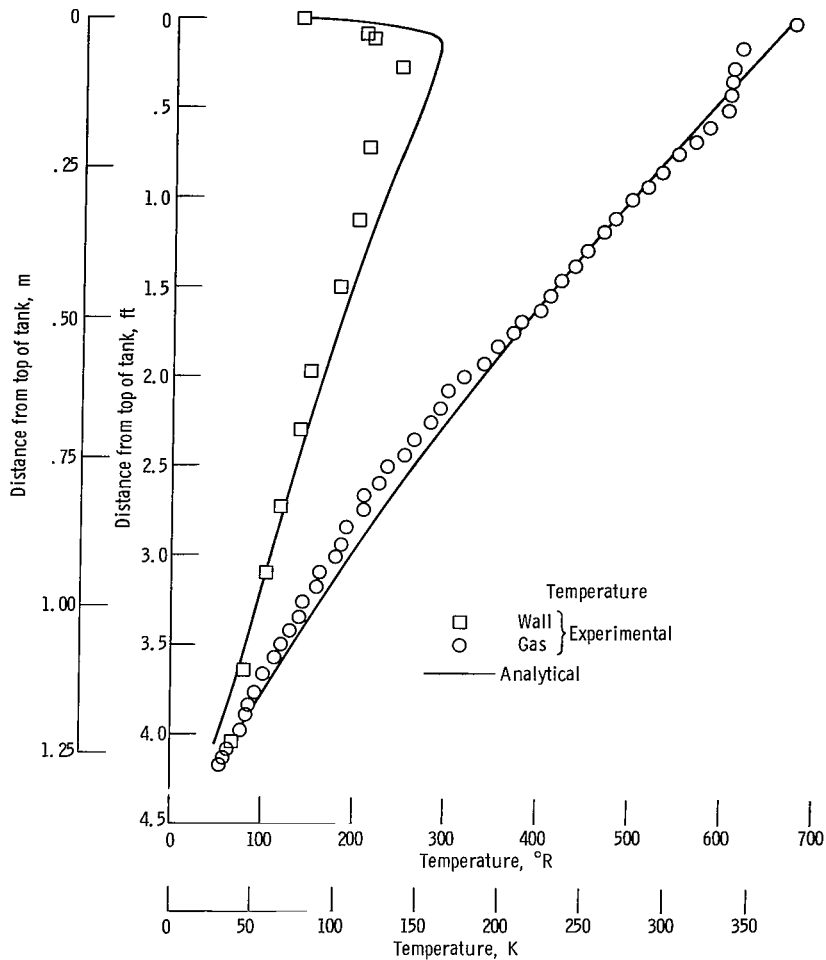
(c) Expulsion time, 134 seconds; inlet gas temperature, 335 K (603° R); run 97.

Figure 16. – Concluded.

served experimentally in the lower 47 percent of the tank ullage but begin to get higher toward the top of the tank. Even though the calculated wall temperatures are higher in the upper portion of the tank wall, the analysis predicts the energy gained by the tank wall (ΔU_w) accurately. The effect of overpredicting the temperatures in the upper portion of the tank wall is offset by an underprediction of the temperature of the tank lid (point zero in fig. 16(a)), which is approximately 22 percent of the total tank mass.

Figure 16(b) is a comparison of experimental and calculated wall and ullage gas temperature profiles at the end of a 137-second expulsion for an inlet gas temperature of 271 K (488° R). Here the calculated gas temperatures agree very closely with the experimental temperatures in the lower 50 percent of the ullage but begin to get lower toward the top of the tank. However, the predicted pressurant requirement is only 1.57 percent higher (lower M_I/M_G) than that observed experimentally.

The calculated wall temperatures agree fairly well with the experimental temperatures except near the top of the tank where they begin to get higher. However, this overprediction is again offset by an underprediction of the lid temperature resulting in an underprediction for wall energy gained of 2.20 percent.

A comparison of experimental and calculated wall and ullage gas temperatures at the end of a 134-second expulsion for an inlet gas temperature of 335 K (603° R) is shown in figure 16(c). Here again there is good agreement between the calculated and experimental gas temperatures throughout the tank ullage resulting in a good prediction for the pressurant requirements (within 2.40 percent). However, in this case the lower calculated lid temperature does not offset the higher calculated wall temperatures in the upper portion of the tank. And the analysis overpredicts the energy gained by the tank wall by 11.31 percent.

The results of these comparisons indicate that the analytical program is able to predict with reasonable accuracy the pressurant gas requirement and the major energy losses for the test conditions imposed herein. The results also indicate that the analytical assumption of a one component ullage (no mass transfer) is adequate and that what hydrogen gas there is in the ullage has little influence on helium pressurant requirements or energy distributions.

Effect of Tank Wall Thickness on Pressurant Requirements

The results of reference 3 indicated that between 77 and 93 percent of the total energy lost by the pressurant gas was lost to the tank wall. It was expected, therefore, that tank wall thickness would play an important role in determining the pressurant requirements during the expulsion period. Additional tests were performed using a 1.52-meter- (5-ft-) diameter spherical tank similar to the one already discussed except the tank wall was chem-milled to an average thickness of 0.409 centimeter (0.161 in.). Although the chem-milling reduced the wall thickness by 46.3 percent, the total weight of the tank was reduced by only 29.5 percent because of the structural requirement of keeping the same thickness for the tank neck, lid, and girth support.

Figure 17 presents a comparison of the M_I/M_G ratio for different expulsion times for the two tank wall thicknesses (0.762 and 0.409 cm; 0.30 and 0.161 in.). Each tank used the hemisphere injector. The average inlet gas temperature for the 0.409-centimeter (0.161-in.) tank was 290 K (~520° R). The average inlet gas temperature for the 0.762-centimeter (0.30-in.) tank was 267 K (~480° R). The 0.409-centimeter- (0.161-in.-) thick tank has an average of 6.3 percent less pressurant requirement, higher M_I/M_G ratio, than the 0.762-centimeter- (0.30-in.-) thick tank for all expulsion times. Similar results were obtained in reference 4 using hydrogen. In all cases, the
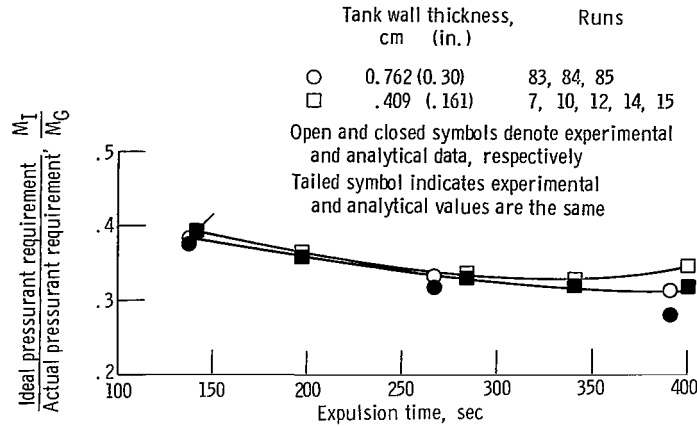
Figure 17. - Comparison of ideal pressurant requirement to actual pressurant requirement ratio as function of expulsion time for two wall thicknesses. Tank pressure, 34.47x10^4 newtons per square meter (50 psia); inlet gas temperature, 277±10 K (499±18° R).

analysis overpredicts the pressurant requirements (underpredicts the M_I/M_G ratio). See table III for deviations between analytical and experimental results.

The 6.3-percent decrease in pressurant requirements was less than expected. However, the test with the 0.409-centimeter- (0.161-in.-) thick tank had an average 23 K (41° R) higher inlet gas temperature. Based on the results already obtained on the effect of inlet gas temperature on pressurant requirements (fig. 9), this 23 K (41° R) higher inlet temperature would normally decrease the pressurant requirement by approximately 2.9 percent. Thus for equal inlet gas temperatures, a nominal decrease in pressurant requirements of approximately 9.0 percent would be expected for the 0.409-centimeter- (0.161-in.-) thick tank.

Figure 18 is a comparison of $\Delta U_w/\Delta U_T$ for different expulsion times for the two tank wall thicknesses. In this figure the $\Delta U_w/\Delta U_T$ ratio is broken down into the fractional portion gained by the tank wall and the total fraction gained by the tank wall plus tank lid. (The tank lid represented 30 percent of the total tank weight for the thinner wall tank compared to 22 percent for the thicker tank.) The fraction of the total energy added that is gained by the tank wall is approximately the same for both tank thicknesses (lower curve of fig. 18) and ranges between 0.37 and 0.40. The values of $\Delta U_w/\Delta U_T$ that include the lid indicate a 4-percent decrease in $\Delta U_w/\Delta U_T$ for the thinner wall tank. It is apparent then that the reduction in the total $\Delta U_w/\Delta U_T$ is almost entirely due to a reduction in the fraction of the total energy absorbed by the lid for the thinner wall tank. The reason for the thinner tank's reduced lid energy gain was that its initial lid temperature, prior to expulsion, was an average of 41 K (73.8° R) higher than the thicker tank's. This higher initial lid temperature reduced the temperature difference between the lid and the ullage gas resulting in less energy gained. The absolute value of the total wall energy gained (table II) by the 0.409-centimeter- (0.161-in.-) thick tank was approximately

32
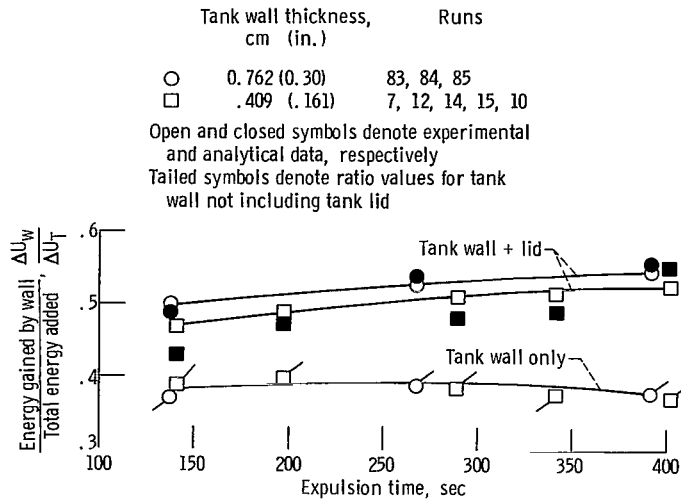
Figure 18. - Comparison of energy gained by wall to total energy added ratio for two tank wall thicknesses. Tank pressure, 34.47×10^4 newtons per square meter (50 psia); inlet gas temperature, 277 ± 10 K ($499° \pm 18°$ R).

6.9 percent less than for the 0.762-centimeter- (0.30-in.-) thick tank.

The absolute values of increase in ullage energy, liquid heating, and mass transfer are approximately the same (within measurement uncertainty) for the two tank wall thicknesses (see tables I and II). Thus, the 6.3-percent reduction in pressurant requirements when using the 0.409-centimeter- (0.161-in.-) thick wall tank is almost entirely due to the 6.9-percent reduction in tank wall heating (ΔU_W).

Pressurant Requirements for Initial Pressurization

The amount of pressurant gas needed to initially pressurize a propellant tank may be important for certain missions, particularly for multiburn missions where the tank is vented after each burn or where the coast period between firings is long enough to enable the ullage gas to collapse.

As stated in the INTRODUCTION, the purpose of this investigation was to determine the capability of the analysis to predict the pressurant requirements during the initial pressurization period as well as the expulsion period. For this purpose, data were collected during the initial pressurization period for various pressurizing rates, inlet gas temperatures, and ullage volumes.

Figure 19 is a comparison of the M_I/M_G ratio as a function of inlet gas temperature for two ramp rates at an initial ullage volume of approximately 4 percent. The data were taken using the hemisphere injector. At constant inlet gas temperature, the pressurant

33
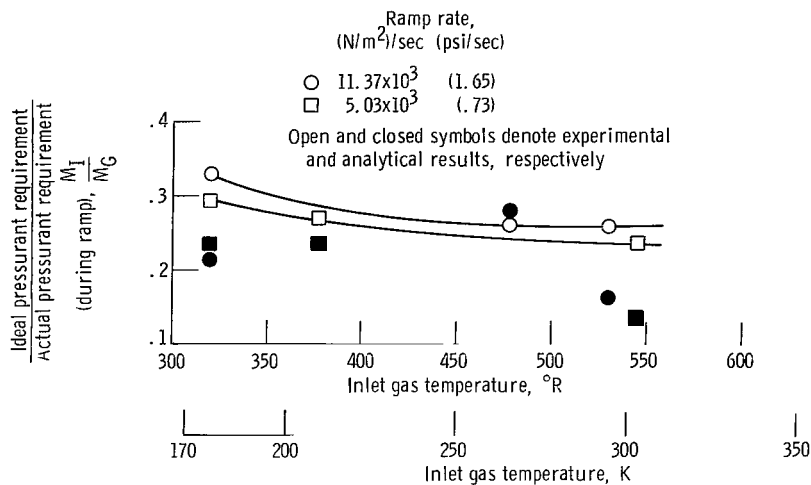
Figure 19. – Comparison of ideal pressurant requirement to actual pressurant requirement ratio for ramp period as function of inlet gas temperature for two ramp rates. Ullage volume, 4 percent.

requirements decreased for increased ramp rates. The M_I/M_G ratio decreases for increasing inlet gas temperature. The reduced pressurant requirements (for the ramp period) for fast ramp rates using low inlet gas temperature is in agreement with the trends during the expulsion period.

The modification of the analysis of reference 1 for the ramp period is discussed in appendix C. As can be seen in figure 19, the analysis is not capable of predicting the pressurant requirements accurately during the initial pressurization of the 4-percent ullage. However, the prediction of the total pressurant requirement (initial pressurization and expulsion) is still adequate because the amount of gas required to pressurize the 4-percent ullage initially was only 4.0 percent (maximum) of the pressurant requirement during expulsion. The absolute pressurant requirements (both experimental and analytical) for the data presented in figures 19 and 20 are given in table IV.

The comparison of M_I/M_G as a function of initial ullage volume for various ramp rates at an inlet gas temperature of approximately 180 K (324° R) is shown in figure 20. This figure indicates increased M_I/M_G for increased ullage volume for any given ramp rate. There is an increased M_I/M_G for increased ramp rates for a given ullage volume. As can be seen in figure 20, the accuracy of the analytical prediction is not consistent. The actual deviation between analytical and experimental values range between 0 and 20.5 percent. The transient process that occurs during the initial pressurization of the tank is too complex to be described by the present analytical model. The analytical program can, however, at least be used to predict the approximate magnitude of pressurant requirements during the ramp period.

Ramp rate,

$(N/m^2)/sec$ (psi/sec)

△ 5.92×10^3 (0.86)
□ 5.03 (.73)
○ 3.24 (.47)

Open and closed symbols denote experimental
and analytical results, respectively
Tailed symbol indicates experimental and
analytical values are the same

$\frac{M_I}{M_G}$

Ideal pressurant requirement (during ramp), / Actual pressurant requirement

Initial ullage volume (percent of total tank volume)
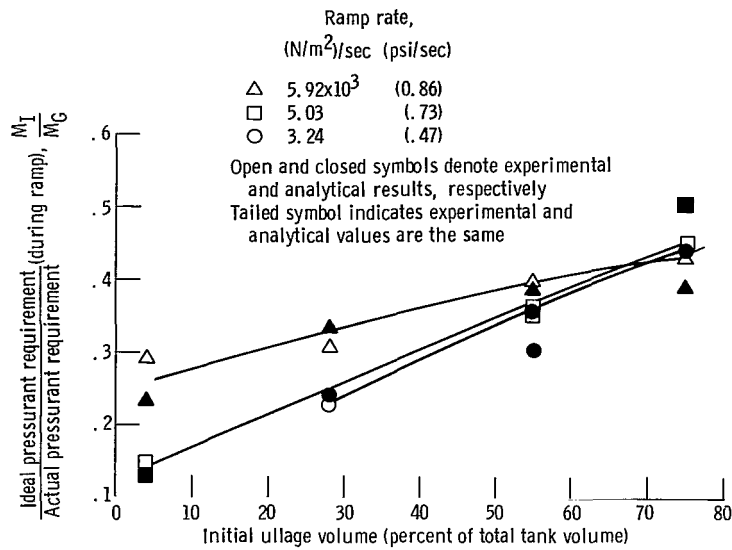
Figure 20. – Comparison of ideal pressurant requirement to actual pressurant requirement ratio for ramp period as function of initial ullage volume for three ramp rates. Inlet gas temperature, 180 K (324° R). Curves are faired through experimental data.

TABLE IV. – COMPARISON OF EXPERIMENTAL AND ANALYTICAL VALUES

OF PRESSURANT GAS REQUIREMENTS FOR RAMP PERIOD

Run	Initial ullage volume, percent	Ramp rate		Mass added				Inlet gas temperature	
		psi/sec	$(N/m^2)/sec$	Experimental		Analytical		K	°R
				lb	kg	lb	kg		
84	4	1.65	11.37×10^3	0.159	0.072	0.148	0.067	265	478
86		.73	5.03	.177	.080	.202	.092	209	377
88		1.65	11.37	.160	.073	.247	.112	178	320
95		1.65	11.37	.110	.050	.175	.079	294	530
96		.73	5.03	.101	.046	.173	.078	302	545
91		.86	5.92	.197	.089	.247	.112	177	319
124	28	.86	5.92	1.344	.610	1.179	.535	181	325
125	28	.47	3.24	1.811	.821	1.701	.772	181	326
147	55	.86	5.92	2.245	1.018	2.312	1.049	174	313
148	55	.73	5.03	2.360	1.070	2.389	1.084	180	323
149	55	.47	3.24	2.257	1.024	2.674	1.213	182	328
394	75	.86	5.92	2.750	1.248	3.054	1.385	169	304
395	75	.73	5.03	2.618	1.188	2.350	1.066	166	299
396	75	.47	3.24	2.522	1.144	2.535	1.150	168	302

SUMMARY OF RESULTS

Tank pressurization and propellant expulsion tests were conducted in 1.52-meter-(5-ft-) diameter spherical tanks to (1) determine what factors have the greatest influence on pressurant gas requirements when using helium as the pressurant, and (2) verify the capability of an analysis to predict the helium pressurant requirements during the initial pressurization period as well as the expulsion period. Tests were conducted using three inlet gas temperatures over a range of liquid outflow rates. The results of this investigation are now given.

Experimental Results

The experimental results indicate an average decrease in helium pressurant gas requirements (M_G) of 1.3 percent for a 10 K (18° R) increase in inlet gas temperature.

Increased inlet gas temperature decreases the residual mass and slightly decreases the energy remaining in the ullage volume after a given expulsion. Of the total energy added to the tank system, between 37.5 and 56.2 percent was lost to the tank wall (of this between 13 and 20 percent was lost to the tank lid) and between 12.8 and 33.7 percent was lost to the liquid.

The mass transfer values obtained in this investigation are inconclusive because of the uncertainty in measuring the ullage gas concentration gradients. Additional work is necessary to develop better techniques for measuring gas concentration gradients and mass transfer.

Decreasing the tank mass by 29.5 percent (by decreasing the tank wall thickness from 0.762 to 0.409 cm; 0.30 to 0.161 in.) decreased the pressurant requirement by an average of 6.3 percent (9.0 percent when corrected for variations in inlet gas temperature).

The effects of inlet gas temperature and ramp rate on the pressurant gas required during the initial pressurization of the tank were as follows:

1. Increased inlet gas temperature decreased the pressurant requirement M_G and mass ratio M_I/M_G for constant ramp rates.

2. Increasing ramp rate decreased the pressurant requirement and increased the mass ratio for constant inlet gas temperatures.

3. Increased pressurant requirement and increased mass ratio were obtained for larger initial ullage volumes for a constant ramp rate.

The trends shown herein for various inlet gas temperatures, liquid outflow rates, and tank wall thickness are consistent with the results obtained using hydrogen as the pressurant (ref. 4). A comparison of the results obtained for the two pressurants indi-

cate that the mass ratios M_I/M_G for similar test conditions are approximately the same. It therefore would require approximately twice as much mass to expel liquid hydrogen using helium as the pressurant instead of hydrogen.

Comparison of Analytical and Experimental Results

The comparison between the analytical and experimental results indicate that, for the range of test conditions used, the analytical program and assumptions are adequate to allow prediction of the pressurant gas requirements during the initial pressurization as well as the expulsion period when using helium as the pressurant. The general results as predicted by the analysis are as follows:

1. The pressurant requirements were predicted to within an average of 4.41 percent for the 322 and 267 K (580° and 480.6^O R) inlet gas temperatures and within 11.46 percent for the 183 K (329° R) inlet gas temperature.

2. Tank wall heating was predicted to within an average of 4.78 percent for all runs.

3. Liquid heating was predicted to within an average of 33.28 percent for all runs.

Lewis Research Center,
  National Aeronautics and Space Administration,
    Cleveland, Ohio, September 22, 1969,
      180-31.

APPENDIX A

INCORPORATION OF A VARIABLE GEOMETRY TO
THE ANALYSIS OF REFERENCE 1

The basic analysis used in this report to predict pressurant gas requirements was developed by W. H. Roudebush in reference 1 for a cylindrical tank.

The major assumptions in the analysis of reference 1 are as follows:

(1) The ullage gas is nonviscous.

(2) The ullage gas velocity is parallel to the tank axis and does not vary radially or circumferentially.

(3) The tank pressure does not vary spatially.

(4) The ullage gas temperature does not vary radially or circumferentially.

(5) The tank wall temperature does not vary radially or circumferentially.

(6) There is no axial heat conduction in either the gas or the wall.

(7) There is no mass transfer (condensation or evaporation).

(8) There is no heat transfer from the pressurant gas to the liquid.

Experiments performed at Lewis (ref. 3) confirmed most of these assumptions when using a diffuser type injector such as the one used herein. The experimental results indicated, however, that there is significant heat transfer from the gas to the liquid with resulting mass transfer.

For the purposes of this report, the analysis of reference 1 was modified for application to arbitrary symmetric tank shapes, and an attempt was made to incorporate the heat transfer from the gas to the liquid. The treatment of internal hardware (e.g., tank baffles, instrumentation) was also modified to correspond to the treatment of heat transfer to the tank wall.

The primary equations which deal with the pressurizing gas upon entering the tank are:

(1) The energy equation

(2) The continuity equation

(3) The equation of heat transfer for a point in the tank wall

ENERGY EQUATION

The form of the energy equation used in the analysis in reference 1 for cylindrical tanks is

$$\frac{\partial T}{\partial t} = \frac{2h_c ZRT}{r\overline{M}PC_p}(T_w - T) - \overline{V}\frac{\partial T}{\partial x} + \frac{RTZ_1}{\overline{M}PC_p}\frac{\partial P}{\partial t} + \frac{RTZ\dot{q}_H C_H}{\pi r^2 \overline{M}PC_p}$$

Modifying this equation to account for both arbitrary symmetric tank shapes and internal tank heat sinks gives

$$\frac{\partial T}{\partial t} = \frac{2h_c ZRT}{r\overline{M}PC_p}(T_w - T)\left[1 + \left(\frac{dr}{dx}\right)^2\right]^{1/2} - \frac{\overline{V}}{}\frac{\partial T}{\partial x} + \frac{RTZ_1}{\overline{M}PC_p}\frac{\partial P}{\partial t} + \frac{\dot{Q}_H}{C_p M_H} \tag{A1}$$

The first term on the right includes the effect of wall curvature. The last term, the energy lost to the internal hardware, is treated as the summation of hardware components: (1) laminated thermoplastic, (2) stainless steel, and (3) copper. For the tanks in this investigation,

$$\frac{\dot{Q}_H}{M_H} = \sum_{\substack{\text{Hardware} \\ \text{components}}} \frac{A_H h_c (T_H - T_G)}{\rho_H V_H} \tag{A2}$$

Gluck and Kline, in reference 8, employed the free convection correlation to the pressurant gas (hydrogen, helium) for the pressurized transfer of liquid hydrogen:

$$\frac{h_c L}{k} = Nu = 0.13\ (GrPr)^{1/3} \tag{A3}$$

This correlation is used herein even though it was developed for cylindrical tanks. Pressurant gas transport properties were evaluated at the mean of the gas and wall temperatures.

CONTINUITY EQUATION (AREA = f(x))

The basic form of the continuity equation for a cylindrical tank is presented in reference 1 (eq. (24)) as

$$\frac{\partial \overline{V}}{\partial x} = \frac{Z_1}{ZT}\left(\frac{\partial T}{\partial t} + \frac{\overline{V}}{}\frac{\partial T}{\partial x}\right) - \frac{Z_2}{ZP}\frac{\partial P}{\partial t}$$

The modified form of the continuity equation due to variations in tank radius with distance along the vertical axis becomes

$$\frac{\partial \overline{V}}{\partial x} = \frac{Z_1}{ZT}\left(\frac{\partial T}{\partial t} + \frac{\overline{V}\,\partial T}{\partial x}\right) - \frac{Z_2}{Z_P}\frac{\partial P}{\partial t} - \frac{2\overline{V}}{r}\frac{\partial r}{\partial x} \tag{A4}$$

where Z_1 and Z_2 are defined in reference 1 as

$$Z_1 = Z + T\left(\frac{\partial Z}{\partial T}\right)_P$$

$$Z_2 = Z - P\left(\frac{\partial Z}{\partial P}\right)_T$$

The last term in equation (A4) evolves from the derivation as follows. For the one-dimensional expression for continuity,

$$\frac{\partial}{\partial x}(\rho\overline{V}A) + \frac{\partial}{\partial t}(\rho A) = 0$$

The substitution $A = \pi r^2$ is made where r is the position radius at location x along the vertical axis:

$$\frac{\partial}{\partial x}(\rho\overline{V}r^2) + \frac{\partial}{\partial t}(\rho r^2) = 0$$

The expression for density from the equation of state $\rho = \overline{M}P/ZRT$ is substituted:

$$P\frac{\partial}{\partial x}\left(\frac{\overline{V}r^2}{ZT}\right) + r^2\frac{\partial}{\partial t}\left(\frac{P}{ZT}\right) = 0$$

The following velocity equation is obtained after performing the partial differentiation and after rearranging terms:

$$\frac{\partial V}{\partial x} = \left[\frac{1}{T} + \frac{1}{Z}\left(\frac{\partial Z}{\partial T}\right)_P\right]\left(\frac{\partial T}{\partial t} + \frac{\overline{V}\,\partial T}{\partial x}\right) + \left[\frac{1}{Z}\left(\frac{\partial Z}{\partial P}\right)_T - \frac{1}{P}\right]\frac{\partial P}{\partial t} - \frac{2\overline{V}}{r}\frac{\partial r}{\partial x}$$

When the expressions involving Z_1 and Z_2 are substituted in this equation, equation (A4) is obtained.

TANK WALL HEAT TRANSFER

Reference 1 (eq. (18)) gives the heat-transfer equation which represents the change in wall temperature as a result of the convective process for a cylindrical tank:

$$\frac{\partial T_w}{\partial t} = \frac{h_c}{l_w \rho_w C_w}(T - T_w) + \frac{\dot{q}_w}{l_w \rho_w C_w} \tag{A5}$$

where $\dot{q}_w$ is the rate of heat addition per unit area to the tank wall from outside the tank. For a small element of volume in the x-direction, equation (A5) can be written as

$$\rho_w C_w V \frac{\partial t_w}{\partial t} = h_c A(T - T_w) + \dot{Q}_w \tag{A6}$$

For a wall of arbitrary shape, the following is evident from the sketch:
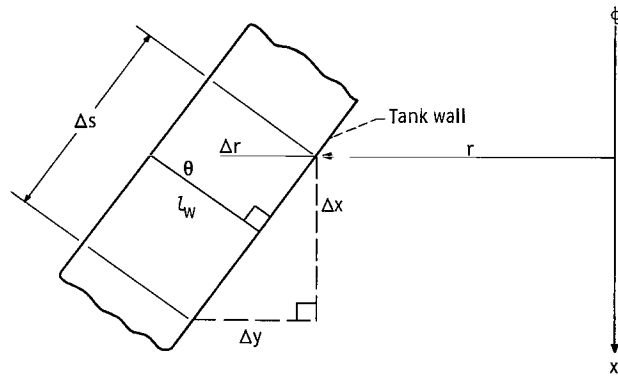
$$\frac{A}{V} = \frac{2\pi r\, \Delta s}{2\pi r\, \Delta r\, \Delta x} = \frac{\Delta s}{\Delta r\, \Delta x} = \frac{1}{l_w}$$

Therefore, equation (A5) holds also for this case.

To account for the large mass concentration at the top of the tank, an equivalent l_w was used. This l_w was obtained by dividing the mass of the tank lid and flange connections by the surface area at the first net point.

41

APPENDIX B

EQUATIONS OF HEAT AND MASS TRANSFER AT THE GAS-LIQUID INTERFACE

The energy and continuity equations (A1) and (A4) should be modified to incorporate both heat transfer from the ullage gas to the liquid surface and mass transfer into the analysis.

The energy equation should incorporate three additional terms:

(1) The heat-transfer rate from the ullage gas to the liquid interface $(\dot{q}_{U \to S})$

(2) The heat-transfer rate from the interface to the liquid $(\dot{q}_{S \to L})$

(3) The energy associated with mass transfer $(\dot{M}_t \lambda)$ (evaporation is positive)

These additional terms can be related by performing an energy balance at the gas-liquid interface as done by W. A. Olsen in reference 9. The resulting energy relation is based on the assumption requiring the interface for a pure system to be at the saturation temperature corresponding to the tank pressure. As shown by the sketch,
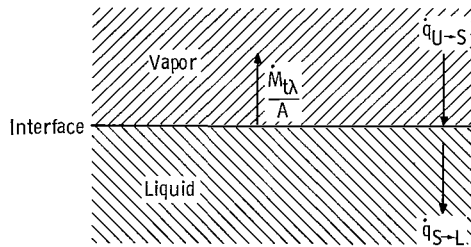
the energy balance at the interface is given by

$$\dot{q}_{U \to S} = \dot{q}_{S \to L} + \frac{\dot{M}_t \lambda}{A}$$

In the case where helium is the pressurant gas for liquid hydrogen, it is assumed that there is sufficient evaporation to maintain a hydrogen blanket over the entire liquid surface. The interface can then be assumed to be at the saturation temperature for a pure hydrogen system.

Experimental data indicat. the energy associated with the mass transfer was relatively small so that the following assumption is made:

$$\frac{\dot{M}_t \lambda}{A} \cong 0$$

With the further qualification that the environmental transfer to the liquid is also small, it follows that

$$\dot{q}_{U \to S} \cong \dot{q}_{S \to L} \cong \frac{d}{dt} (U_L) \tag{B2}$$

The term $\frac{d}{dt} (U_L)$ can be determined from experimental data. The analysis requires that $\dot{q}_{U \to S}$ must be related to the ullage gas variables. This is done by the following equation which involves defining a heat-transfer coefficient $(h_{c, L})$ and a temperature (T_δ) somewhere in the vapor:

$$\dot{q}_{U \to S} \equiv h_{c, L}(T_\delta - T_{sat}) \tag{B3}$$

The flow process is free convection flow of pressurant gas essentially down the tank wall and then radially inward across the liquid surface.

With regard to $h_{c, L}$, reference 10 develops an equation from boundary layer theory for forced flow across a horizontal, semi-infinite, constant temperature flat plate given by

$$Nu = \frac{h_{c, L} L}{k} = 0.664 \left(\frac{\mu C_p}{k} \right)^{1/3} \left(\frac{L \overline{V}_L \rho}{\mu} \right)^{1/2} \tag{B4}$$

The velocity $\overline{V}_L$ of the gas across the liquid surface in terms of the gas velocity $\overline{V}_G$ down a vertical wall is given in reference 11 as

$$\overline{V}_L = 0.0975 \, \overline{V}_G \tag{B5}$$

where $\overline{V}_G$, obtained by solving the integrated energy and momentum equations at the wall boundary, is given by

$$\overline{V}_G = 1.185 \frac{\mu}{\rho Z} \frac{Gr^{1/2}}{\left(1 + 0.494 \, Pr^{2/3} \right)^{1/2}} \tag{B6}$$

Combining equations (B5) and (B6) for $\overline{V}_L$ and substituting into (B4) gives

$$Nu = \frac{h_{c, L} L}{k} = \frac{0.226 \, Pr^{1/3} \, Gr^{1/4}}{\left(1 + 0.494 \, Pr^{2/3} \right)^{1/4}} = 0.21 \, Pr^{1/3} \, Gr^{1/4} \tag{B7}$$

for a value of Pr between 0.74 and 0.90. Equation (B7) is similar in form to the empir-

ical relation for free convection flow along vertical planes and cylinders given in reference 12 as

$$Nu = \frac{h_{c,L} L}{k} = n(Gr\,Pr)^m \tag{B8}$$

Equation (B8) is used herein with exponent $m = 1/3$ and a multiplier $n = 0.14$ because it is simpler and fits the data somewhat better than equation (B7).

At this point, some choice of T_δ that is consistent with the definition of $h_{c,L}$ and fits the data for $\dot{q}_{U\rightarrow S}$ (i.e., $\frac{d}{dt}(U_L)$) must be made. In reference 13, liquid hydrogen was pressurized with a low mixing diffuser and no liquid outflow. The adiabatic compression temperature given by $T_{ad} = T_0\,(P/P_0)^{(\gamma-1)/\gamma}$ was used as the choice for T_δ. This relation gave good agreement between analytical and experimental mass flux results for hydrogen pressurant. For the conditions described in reference 13, appreciable condensation occurred. Reference 13 indicates that as T_δ increased, there was a tendency toward evaporation, away from the condensation results that occurred when the adiabatic temperature was used. With greater ullage gas mixing (due to diffuser characteristics as well as the liquid outflow process), T_δ would be expected to be greater than T_{ad}. For the work described in this report, T_δ was obtained from the following relation evaluated with experimental data:

$$\dot{q}_{U\rightarrow S} = h_{c,L}\,(T_\delta - T_{sat}) = \frac{d}{dt}\,U_L$$

One experimental run, where the expulsion time was 271 seconds (run 95), was used for the determination of T_δ where $h_{c,L}$ is given by (B8). For this condition T_δ was determined to be 1.3 times the adiabatic compression temperature or 46.3 K (83.3° R) for a tank pressure of 34.47×10^4 newtons per square meter (50 psia). For convenience this value of T_δ was used for all comparisons since the effect of the interfacial terms in the energy equation was small in the experimental situation.

Using equation (B8), as well as the values for T_δ and T_{sat} discussed previously, gave the final form of the equation used to evaluate the heat transferred from the ullage gas to the liquid interface as follows:

$$\dot{q}_{U\rightarrow S} = \frac{k}{L}\,(0.14)(Gr\,Pr)^{1/3}\,(46.3\ K - T_{sat}) \tag{B9}$$

In order to incorporate liquid heating to the analysis the term

$$-\frac{\dot{q}_{U \to S}\, A_L}{X_n V \rho} \quad \text{or} \quad -\frac{k(0.14)(\mathrm{GrPr})^{1/3}\,(46.3\ \mathrm{K} - T_{sat}) \cdot A_L}{L X_n V \rho} \tag{B10}$$

must be added to the right side of equation (A1).

APPENDIX C

RAMP ANALYSIS

The amount of pressurant gas needed to pressurize a propellant tank initially may be important for multiburn missions. When the coast period between firings is long, a collapse in ullage pressure may develop. Under these circumstances a significant amount of pressurant may be necessary to repressurize the propellant tank for the next firing.

An application of the work reported in reference 1 is the prediction of the pressurant requirements for the initial pressurization (ramp) and hold periods. A separate computer program, which determines the pressurant as well as energy requirements during the ramp and hold periods, is described herein. The same equations which describe the expulsion period, as outlined in appendix A, are also applicable for the ramp and hold periods. However, the ramp period is more difficult to model analytically than the expulsion period, particularly for small ullage volumes where the liquid surface is near the injector outlet. Even though the experimental results indicated relatively large amounts of mass transfer during this period, the incorporation of mass transfer into the ramp analysis was not attempted because of the added complexity and incomplete knowledge of the mass transfer phenomenon. The heat transfer from the ullage to the liquid surface is also neglected in the analytical model for the ramp period.

The analysis used for the ramp period computes the gas temperatures in the ullage at any time during the pressure rise from the gas energy equation. The corresponding gas velocities are computed from the equation of continuity. The iterative method to be described shows how convergence is achieved in the solution of the gas energy and continuity equations. The predicted mass of pressurant is based on an integration of the volume elements in the ullage at the end of the ramp and hold periods assuming a one component ullage (100 percent helium). Quantitatively, the entire mass of pressurant requirements for the ramp period was less than the expulsion period by a factor of 30 to 60 when the initial ullage was 4 percent of the tank volume.

INPUT DATA REQUIREMENTS

For the solution to proceed, a set of boundary and initial conditions are required. These conditions, which are the same for the expulsion as well as the pressurization, are as follows:

(1) At time $t = 0$, the values of gas temperature T and wall temperature T_w as functions of x, the position within the ullage

(2) On the boundary $x = 0$, the value of inlet gas temperature T as a function of time

(3) At the liquid surface, the value of gas temperature T, wall temperature T_w, and velocity $\overline{V}$ as functions of time (Although movement of the interface has been noted during the ramp pressurization period, no significant effect on the programed output was noted with the value of $\overline{V} = 0$ at the interface.)

(4) Tank pressure P, outside heating rate $\dot{q}_w$, inside hardware heating rate $\dot{q}_H$ as a function of time (Like the other initial conditions, the pressure P as a function of time or ramp pressure curve is defined by a discrete set of points which approximate a smooth curve. In regions of pronounced curvature, more points are needed for accurate definition than for linear portions.)

(5) Constant value of heat-transfer coefficient h_c, or a correlating equation from which h_c may be evaluated at each net point from values of T, T_w, and P

(6) Tank radius as function of axial distance down from the top of the tank

(7) Tank wall material properties: density ρ_w and specific heat $C_w(T_w)$

(8) Tank wall thickness (average membrane plus weld area thickness) as function of axial distance down from the top of the tank

(9) Pressurizing gas properties: Molecular weight $\overline{M}$, specific heat $C_p(T)$, and compressibility factor $Z(P, T)$

(10) Initial ullage height, total time of run, the number of net points in the initial ullage space

(11) The initial time step Δt used in following the pressure rise as well as establishing the points of computation

(12) If the hold period is to be included in the analysis, then the time for the end of the ramp must be specified

APPLICATION OF BASIC EQUATIONS

Reference 1 makes the substitution of $T_{w,i}$ from the finite difference form of equation (A6) into the finite difference form of the energy equation. Rearranging gives a quadratic in the gas temperature T_i' where the prime refers to a step forward in time and the quantities without the prime are evaluated at the previous time step:

$$T_i'^2 + \left[\alpha_i^*\left(1 + \overline{V}_i^* \frac{\Delta t}{\Delta x} - \omega_i^*\right) - T_{w,i} - \left(\frac{\dot{q}_w \Delta t}{l_w \rho_w C_w}\right)_i^*\right]T_i' - \alpha_i^*\left(\overline{V}_i^* \frac{\Delta t}{\Delta x} T_{i-1}' + T_i\right) = 0 \qquad (C1)$$

The quantity marked with the asterisk may be evaluated either at the beginning or the end of the time interval.

A difficulty can arise when evaluating the gas energy equation expressed by the pre-

vious quadratic. This occurs when the heat transfer takes place from the wall into the ullage gas. For this situation, the solution of the continuity equation provided negative gas velocities which made it impossible for equation (C1) to converge on the real roots.

At the start of the ramp (immediately after filling the tank), the initial wall temperature distribution in the ullage is higher than the gas temperature distribution. This is brought about since the wall surface above the liquid is exposed to the ambient temperature. But the ullage gas temperature near the liquid interface is close to the saturation temperature at 1 atmosphere.

The technique used when $T_{w,i} > T_i$ involved a direct substitution. The finite difference form of equation (A4) is

$$
\overline{V}'_i = \frac{T'_i \overline{V}'_{i+1} - \left(\frac{Z_1}{Z}\right)'_i \left(\frac{\Delta x}{\Delta t}\right)\left(T'_i - T_i\right) + \left(\frac{Z_2}{Z}\right)'_i \frac{T'_i}{P'} \frac{\Delta x}{\Delta t} (P' - P)}{T'_i + \left(\frac{Z_1}{Z}\right)'_i \left(T'_{i+1} - T'_i\right) - 2 \frac{\Delta x}{r_i} T'_i \left(\frac{\Delta r}{\Delta x}\right)} \tag{C2}
$$

Combining the equations involving ullage gas temperature T'_i and velocity $\overline{V}'_i$, equations (C1) and (C2), gives the following cubic results:

$$
b_i T'^3_i + \left[\left(\frac{Z_1}{Z}\right)'_i T'_{i+1} + b_i c_i + \alpha^*_i \frac{\Delta t}{\Delta x}\left(\overline{V}'_{i+1} + d_i\right)\right] T'^2_i
$$

$$
+ \left[c_i \left(\frac{Z_1}{Z}\right)'_i T'_{i+1} + \alpha^*_i \frac{\Delta t}{\Delta x}\left(\frac{Z_1}{Z}\right)'_i \frac{\Delta x}{\Delta t} T_i - \alpha^*_i \frac{\Delta t}{\Delta x} T'_{i-1}\left(\overline{V}'_{i+1} + d_i\right) - \alpha^*_i T_i \frac{\Delta t}{\Delta x} b_i\right] T'_i
$$

$$
- \alpha^*_i \frac{\Delta t}{\Delta x}\left(\frac{Z_1}{Z}\right)'_i \frac{\Delta x}{\Delta t} T_i T'_{i-1} - \alpha^*_i T_i \left(\frac{Z_1}{Z}\right)'_i T'_{i+1} = 0 \tag{C3}
$$

This arrangement of terms eliminates V'_i and the cubic is solved for the gas temperature T'_i.

ANALYTICAL PROCEDURE

The analytical procedure uses a variable time increment Δt in following the pressure rise. With this technique, the iteration was stable over a range of inlet conditions

and the results were consistent with the recorded data.

First, the velocity distribution is determined in the initial ullage at time $t = 0$. The substituted form of equation (A4) (in which the energy equation (A1) is substituted for $\partial T / \partial t$) is put into finite difference form and solved for the velocity distribution for the first time.

For most of the ramp runs encountered in this investigation, an initial time increment of 1 second proved satisfactory.

TEMPERATURE CALCULATIONS FROM TOP TO INTERFACE

Since values of $\overline{V}$ have been obtained at each net point at time $t = t_1 = 0$, attention is turned to equation (C3) which is cubic in T_i'. During the iteration, the cubic equation (C3) is solved for the gas temperature T_i' starting at the point N_2 in figure 21.
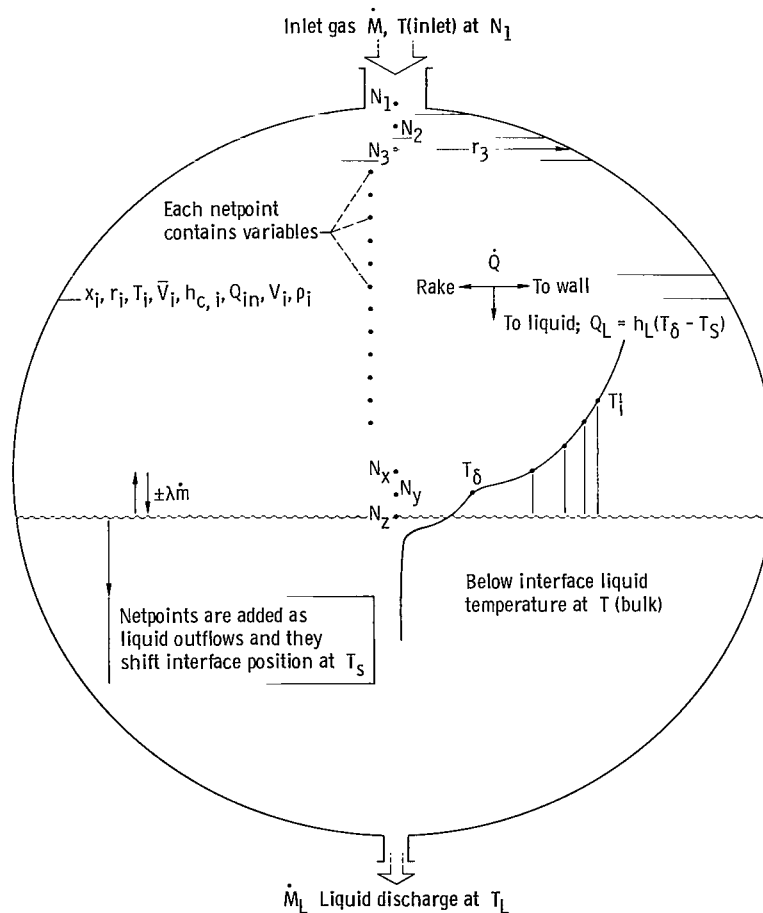
Figure 21. – Analytical model. (Coordinate system is positive in downward direction from $x = 0$ at N_1 to $x = n$ at interface N_z.)

When this equation is first solved for the ullage temperature distribution, a value for T'_{i+1} is not available. A substituted value of T_{i+1} proved to be satisfactory as an initial guess to get convergence. All other quantities in equation (C3) are available from the initial conditions. The value for T'_{i-1}, the temperature at N_1, is known as a boundary condition.

The solution for T'_i at N_3 follows, and this procedure continues to calculate gas temperatures until the boundary at the interface is reached. The values for the corresponding wall temperatures are calculated using the finite difference form of equation (A6).

VELOCITY CALCULATIONS FROM INTERFACE TO TOP

Although the ullage temperatures are computed starting at the top (fig. 21), the velocity equation (C2) is used to calculate the ullage gas velocity starting with the point N_y near the interface. The velocity at the interface N_z, the boundary value, is zero with no expulsion.

The ullage gas velocity is calculated from point to point until the top of the tank is reached. The new velocities are used in equation (C3) along with previous values of T'_{i+1} and the temperature distribution is redetermined. This process is continued until convergence is achieved over the entire ullage. The time is advanced to t_2 and a new set of velocities is determined.

COMPLETING THE SOLUTION

With the new velocities at time t_2, we evaluate equation (C3) again starting at point N_2 and terminating at the interface. A value for T'_{i+1} is always available from the previous iteration, although a substituted value of T_{i+1} is used as the first value.

The new values for T'_i at all the points for time t_2 are used to recompute the velocity distribution. This new set of velocities is then compared with the previous set and convergence is assumed if the deviation is less than half of 1 percent for every velocity in the time set. A time step is then taken to t_3.

If convergence is not achieved after 40 iterations, the time step is reduced and the iteration process is reinitiated. Generally the reduction in time step becomes necessary only when there is a severe change in the slope of the ramp curve particularly in the early stages of the pressure rise.

For the new time t_3, the temperature T'_i in equation (C3) is determined from the converged value using the iterating method. This procedure continues to evaluate the

gas temperatures and velocity distribution in the ullage for each time step taken in following the rate of pressure in the tank.

The initial gas velocity distribution used in solving equation (C3) for each new time t is obtained from the previous time as follows:

$$V_{t,2} = V_{t,1} \frac{\left(\dfrac{\Delta P_{1-2}}{\Delta t_{1-2}}\right)}{\left(\dfrac{\Delta P_{0-1}}{\Delta t_{0-1}}\right)} \tag{C4}$$

This iterative procedure can be used for a constant pressure representing the hold period. However, for initiating the ramp, an actual pressure rise must be used. A typical example is shown in figure 22.
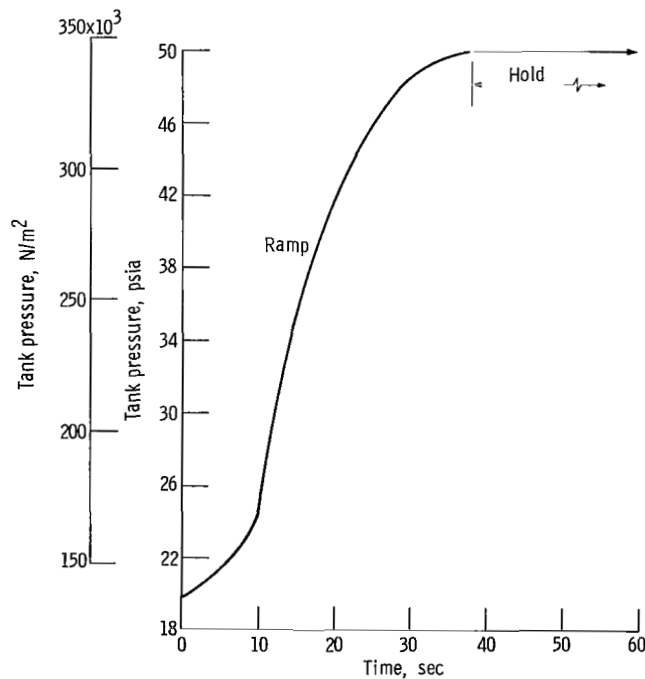
Figure 22. – Tank pressure as function of time during initial pressurization period for run 96.

APPENDIX D

DATA REDUCTION

PHYSICAL DESCRIPTION OF PROBLEM

An initially vented tank containing two-phase hydrogen was pressurized from 1 atmosphere to a new pressure by adding helium gas. The system was then allowed to stabilize at which time liquid outflow was started. During this expulsion period, pressurant gas (helium at constant temperature) was added to the tank at a rate that maintained a constant tank pressure while expelling the liquid at a desired rate. The amount of pressurant gas used during the expulsion phase is dependent on (1) the volume of liquid displaced with no heat or mass transfer, (2) the heat transfer to the tank wall and liquid, (3) the amount of mass condensed or evaporated, and (4) the amount of helium gas absorbed by the liquid hydrogen.

The main parameter used in the comparisons was the ratio of the ideal pressurant requirement to the actual pressurant requirement. The ideal pressurant was determined under the assumption that the incoming pressurant gas did not exchange energy or mass with the surroundings. Under this assumption, the ideal pressurant required for the initial pressurization of the tank was determined by the adiabatic relation

$$M_I = \frac{\overline{M}P_o V_o}{ZRT_G}\left[\left(\frac{P_f}{P_o}\right)^{1/\gamma} - 1\right] \tag{D1}$$

The ideal pressurant required for the expulsion period was determined by the relation

$$M_I = \frac{\overline{M}P \Delta V_U}{ZRT_G} \tag{D2}$$

MASS BALANCE

A mass balance was performed on the ullage volume from an initial time t_i to a final time t_f as follows:

$$M_{U,f} = M_{U,i} + M_{G,i \rightarrow f} \pm M_{t,i \rightarrow f} \tag{D3}$$

A discussion of how the terms of equation (D3) were determined follows.

Pressurant Gas Added ($M_{G, i \to f}$)

The weight of the actual pressurant gas added from any initial time t_i to any final time t_f was determined by numerical integration of the gas orifice equation

$$M_{G, i \to f} = \int_{t_i}^{t_f} YD^2C \sqrt{\rho \, \Delta P^*} \; dt \qquad\qquad (D4)$$

The time necessary to expel ΔV_U of liquid is $(t_f - t_i)$.

Ullage Mass

The initial ullage mass $M_{U, i}$ and final ullage mass $M_{U, f}$ were obtained by numerical integration of the particular density profiles:

$$M_{U, i} = \int_{V_{U, i}} \rho \; dV \simeq \sum_{n=1}^{N_i} \rho_n V_n \qquad \text{where} \quad \rho = f\left(T, X_{H_2}, X_{He}\right) \qquad (D5)$$

$$M_{U, f} = \int_{V_{U, f}} \rho \; dV \simeq \sum_{n=1}^{N_f} \rho_n V_n \qquad \text{where} \quad \rho = f\left(T, X_{H_2}, X_{He}\right) \qquad (D6)$$

The internal tank volume was considered as 57 (corresponding to thermopile location) horizontal disk segments. Each of these segments was in turn divided radially into a series of concentric rings, the number of which depended on location of radial temperature sensors and the vertical position of the disk segment being considered. These rings (339 in all) comprised the V_n's in the previous calculations. In this manner, vertical temperatures as well as radial temperature gradients could be incorporated into the mass calculations. The position of the liquid level prior to and after expulsion determined the number of gas volume rings (N_i and N_f) used in the ullage mass calculations. The density of the two component ullage was calculated from the Beattie-Bridgeman equation of state for a mixture given in reference 14 as

$$P = \frac{RT(1 - \epsilon)}{\overline{M}'v^2} (v + B_T) - \frac{A_T}{v^2} \qquad\qquad (D7)$$

where

$$A_T = \left(X_{H_2}\sqrt{A_{H_2}} + X_{He}\sqrt{A_{He}}\right)^2 \left(1 - \frac{X_{H_2}a_{H_2} + X_{He}a_{He}}{v}\right)$$

$$B_T = \left(X_{H_2}B_{H_2} + X_{He}B_{He}\right)\left(1 - \frac{X_{H_2}b_{H_2} + X_{He}b_{He}}{v}\right)$$

and

$$\epsilon = \frac{X_{H_2}C_{H_2} + X_{He}C_{He}}{vT^3}$$

Equation (D7) can then be solved for $\frac{1}{v_n}$ (where $\frac{1}{v_n} = \rho_n$) by knowing the pressure, temperature, and ullage gas concentration for each ΔV_n segment.

Mass Transfer

The mass transfer was calculated from equation (D3) as a result of knowing $M_{U,f}$, $M_{U,i}$ and $M_{G,i \to f}$; that is,

$$M_{t,i \to f} = M_{U,i} + M_{G,i \to f} - M_{U,f} \tag{D8}$$

If $M_{t,i \to f}$ was a positive quantity, mass was considered leaving the ullage volume (e.g., condensation and/or absorption).

ENERGY BALANCE

For the thermodynamic system consisting of the entire tank and its contents (tank + ullage gas + liquid), the first law of thermodynamics for an increment of time dt may be written as

$$dU_T = (\delta M_G)\left(u_G + P_G v_G + \frac{\overline{V}_G^2}{2g} + z_G\right) - (\delta M_L)\left(u_L + P_L v_L + \frac{\overline{V}_L^2}{2g} + z_L\right) + \delta Q - \delta W$$

$$\tag{D9}$$

The kinetic and potential energy terms are small in comparison with the other energy terms and are neglected in this development. If $h = u + Pv$ is substituted, equa-

tion (D9) becomes

$$dU_T = (\delta M_G)h_G - (\delta M_L)h_L + \delta Q - \delta W \qquad (D10)$$

For this system, there is no external work done so $\delta W = 0$ and the final form of equation (D9) therefore becomes

$$dU_T = (\delta M_G)h_G - (\delta M_L)h_L + \delta Q \qquad (D11)$$

Equation (D11) can be integrated over any time period. The physical interpretation of the quantities in equation (D11) is as follows:

$$\underbrace{\int_{U_i}^{U_f} dU_T}_{\substack{\text{Change in} \\ \text{system} \\ \text{energy} \\ \text{(Tank + Gas} \\ \text{+ Liquid)}}} = \underbrace{\int_{t_i}^{t_f} \dot{M}_G h_G \, dt}_{\substack{\text{Energy input} \\ \text{by pressurant} \\ \text{gas inflow}}} - \underbrace{\int_{t_i}^{t_f} \dot{M}_L h_L \, dt}_{\substack{\text{Energy leaving} \\ \text{through} \\ \text{liquid outflow}}} + \underbrace{\int_{t_i}^{t_f} \dot{Q} \, dt}_{\substack{\text{Energy from} \\ \text{environment} \\ \text{(heat leak from} \\ \text{conduction,} \\ \text{convection and} \\ \text{radiation)}}} \qquad (D12)$$

A discussion of how the terms of equation (D12) were evaluated follows.

Energy Input by Pressurant Gas in Flow

The first term in equation (D12) may be evaluated as follows:

$$\int_{t_i}^{t_f} \dot{M}_G h_G \, dt \simeq \sum_{n=0}^{n=\frac{t_f - t_i}{\Delta t}} \dot{M}_{G,n} h_{G,n} \, \Delta t \qquad (D13)$$

The pressurant flow rate $\dot{M}_G$ was determined from equation (D4). The specific enthalpy of the inlet gas was evaluated at the inlet temperature and pressure at each time increment Δt.

Energy Leaving by Liquid Outflow

The energy of the liquid that leaves the system can be evaluated as follows:

$$\int_{t_i}^{t_f} \dot{M}_L h_L \, dt \simeq \sum_{n=0}^{n=\frac{t_f - t_i}{\Delta t}} M_{L,n} h_{L,n} \, \Delta t \tag{D14}$$

The liquid flow rate $\dot{M}_L$ was determined from the turbine flowmeter. The specific enthalpy of the liquid was evaluated at the outlet temperature.

Energy Input from Environment

The rate of energy input into the tank from the environment was assumed to be the same for all cases and was determined from a boiloff test. This test indicated a nominal value of 0.732×10^3 joules per second (0.694 Btu/sec) should be used. This value, which includes heat input by radiation, convection, and conduction through pipes and supports, was in all test cases less than 7.0 percent of the energy added to the tank by the pressurant gas:

$$\int_{t_i}^{t_f} \dot{Q} \, dt \simeq 0.732 \times 10^3 \, (t_f - t_i) \tag{D15}$$

Change in System Energy

The change in system energy can be separated into three categories: (1) change in ullage energy, (2) change in liquid energy, and (3) change in the wall energy. Stated mathematically,

$$dU_T = dU_U + dU_L + dU_W \tag{D16}$$

Change in Ullage Energy

The change in the ullage energy over any given time interval $(t_i \rightarrow t_f)$ is obtained by subtracting the internal energy of the ullage at time t_i from the internal energy at time t_f:

56

$$\int_{U_{t_i}}^{U_{t_f}} dU_U = \left(U_U\right)_{t_f} - \left(U_U\right)_{t_i} \tag{D17}$$

Making use of the relation $U = H - PV$ gives

$$\int_{U_{t_i}}^{U_{t_f}} dU_U = \sum_{V_f} \rho_U \left(h - \frac{P}{\rho_U}\right)\Delta V_U - \sum_{V_i} \rho_U \left(h - \frac{P}{\rho_U}\right)\Delta V_U \tag{D18}$$

The ullage gas density was determined using equation (D7). The ullage gas enthalpy was calculated using the relation

$$h = \frac{M_{H_2}}{M_T} h_{H_2} + \frac{M_{He}}{M_T} h_{He} \tag{D19}$$

Therefore, since the pressure and temperature and ullage gas concentration profiles at times t_f and t_i were known, the change in ullage energy was evaluated.

Change in Liquid Energy

The change in energy of the liquid in the tank can be determined in a manner similar to the change in ullage energy:

$$\int_{U_{t_i}}^{U_{t_f}} dU_L = \left(U_L\right)_{t_f} - \left(U_L\right)_{t_i} \tag{D20}$$

or

$$\int_{U_{t_i}}^{U_{t_f}} dU_L = \sum_{V_f} \rho_L \left(h_L - \frac{P}{\rho_L}\right)\Delta V_L - \sum_{V_i} \rho_L \left(h_L - \frac{P}{\rho_L}\right)\Delta V_L \tag{D21}$$

where the liquid density and enthalpy are functions of pressure and temperature.

Change in Wall Energy

The change in wall energy was determined by applying the first law of thermodynamics to an element of the wall:

$$\int_{U_{t_i}}^{U_{t_f}} dU_w = \Delta U_w = \Delta M_w \int_{T_1}^{T_2} C_v\, dT \qquad \text{where} \quad C_v = C_v(T) \qquad (D22)$$

The total change of the wall is then

$$\Delta U_{w,T} \cong \sum_{M_w} \Delta U_w \cong \sum_{M_w} \Delta M_w \int_{T_1}^{T_2} C_v(T) dT \qquad (D23)$$

Total Energy Change of System

For convenience equation (D16) is substituted into (D12):

$$\int_{t_i}^{t_f} \frac{d}{dt}[U_U + U_w + U_L] dt = \int_{t_i}^{t_f} \dot{M}_G h_G\, dt - \int_{t_i}^{t_f} \dot{M}_L h_L\, dt + \int_{t_i}^{t_f} \dot{Q}\, dt \qquad (D24)$$

Rearranging terms gives

$$\underbrace{\int_{t_i}^{t_f} [\dot{M}_G h_G + \dot{Q}] dt}_{} = \underbrace{\int_{t_i}^{t_f} [\dot{M}_L h_L\, dt + dU_L]}_{} + \underbrace{\int_{t_i}^{t_f} dU_U}_{} + \underbrace{\int_{t_i}^{t_f} dU_w}_{} \qquad (D25)$$

| Total energy added (ΔU_T) | Total change in liquid in tank plus liquid expelled energy (ΔU_L) | Total change in ullage energy (ΔU_U) | Total change in wall energy (ΔU_w) |

Dividing through by ΔU_T gives

$$1 = \frac{\Delta U_L}{\Delta U_T} + \frac{\Delta U_U}{\Delta U_T} + \frac{\Delta U_w}{\Delta U_T} \qquad (D26)$$

The data presented herein are in the form of these ratios which show the relative distribution of the total energy input.

REFERENCES

1. Roudebush, William H.: An Analysis of the Problem of Tank Pressurization During Outflow. NASA TN D-2585, 1965.

2. Epstein, M.; Georgius, H. K.; and Anderson, R. E.: A Generalized Propellant Tank-Pressurization Analysis. International Advances in Cryogenic Engineering. Vol. 10. K. D. Timmerhaus, ed., Plenum Press, 1965, pp. 290-302.

3. DeWitt, Richard L.; Stochl, Robert J.; and Johnson, William R.: Experimental Evaluation of Pressurant Gas Injectors During the Pressurized Discharge of Liquid Hydrogen. NASA TN D-3458, 1966.

4. Stochl, Robert J.; Masters, Phillip A.; DeWitt, Richard L.; and Maloy, Joseph E.: Gaseous-Hydrogen Requirements for the Discharge of Liquid Hydrogen from a 1.52-Meter- (5-foot-) Diameter Spherical Tank. NASA TN D-5336, 1969.

5. Stochl, Robert J.; Masters, Phillip A.; DeWitt, Richard L.; and Maloy, Joseph E.: Gaseous-Hydrogen Pressurant Requirements for the Discharge of Liquid Hydrogen from a 3.96-Meter- (13-foot-) Diameter Spherical Tank. NASA TN D-5387, 1969.

6. Stochl, Robert J.; and DeWitt, Richard L.: Temperature and Liquid-Level Sensor for Liquid-Hydrogen Pressurization and Expulsion Studies. NASA TN D-4339, 1968.

7. Roellig, Leonard O.; and Giese, Clayton: Solubility of Helium in Liquid Hydrogen. J. Chem. Phys., vol. 37, no. 1, July 1, 1962, pp. 114-116.

8. Gluck, D. F.; and Kline, J. F.: Gas Requirements in Pressurized Transfer of Liquid Hydrogen. Advances in Cryogenic Engineering. Vol. 7. K. D. Timmerhaus, ed., Plenum Press, 1962, pp. 219-233.

9. Olsen, William A., Jr.: Analytical and Experimental Study of Three Phase Heat Transfer with Simultaneous Condensing and Freezing on Cold Horizontal and Vertical Plates. Ph.D. Thesis, Univ. Connecticut, 1967.

10. Kays, W. M.: Convective Heat and Mass Transfer. McGraw-Hill Book Co., Inc., 1966.

11. Dickson, Philip F.: Large Gradient Mass Transfer. Ph.D. Thesis, Univ. Minnesota, 1962.

12. McAdams, William H.: Heat Transmission. Third ed., McGraw-Hill Book Co., Inc., 1954.

13. Olsen, William A.: Experimental and Analytical Investigation of Interfacial Heat and Mass Transfer in a Pressurized Tank Containing Liquid Hydrogen. NASA TN D-3219, 1966.

14. Dodge, Barnett F.: Chemical Engineering Thermodynamics. McGraw-Hill Book Co., Inc., 1944, pp. 183-186.

"*The aeronautical and space activities of the United States shall be conducted so as to contribute . . . to the expansion of human knowledge of phenomena in the atmosphere and space. The Administration shall provide for the widest practicable and appropriate dissemination of information concerning its activities and the results thereof.*"

— NATIONAL AERONAUTICS AND SPACE ACT OF 1958

NASA SCIENTIFIC AND TECHNICAL PUBLICATIONS

TECHNICAL REPORTS: Scientific and technical information considered important, complete, and a lasting contribution to existing knowledge.

TECHNICAL NOTES: Information less broad in scope but nevertheless of importance as a contribution to existing knowledge.

TECHNICAL MEMORANDUMS: Information receiving limited distribution because of preliminary data, security classification, or other reasons.

CONTRACTOR REPORTS: Scientific and technical information generated under a NASA contract or grant and considered an important contribution to existing knowledge.

TECHNICAL TRANSLATIONS: Information published in a foreign language considered to merit NASA distribution in English.

SPECIAL PUBLICATIONS: Information derived from or of value to NASA activities. Publications include conference proceedings, monographs, data compilations, handbooks, sourcebooks, and special bibliographies.

TECHNOLOGY UTILIZATION PUBLICATIONS: Information on technology used by NASA that may be of particular interest in commercial and other non-aerospace applications. Publications include Tech Briefs, Technology Utilization Reports and Notes, and Technology Surveys.

Details on the availability of these publications may be obtained from:

SCIENTIFIC AND TECHNICAL INFORMATION DIVISION

NATIONAL AERONAUTICS AND SPACE ADMINISTRATION

Washington, D.C. 20546